



**Cite this:** *RSC Appl. Polym.*, 2023, **1**, 204

## Recent advances in thermogels for the management of diabetic ocular complications

Nicholas Wei Xun Ong, <sup>a,b,c</sup> Belynn Sim, <sup>a,c</sup> Jun Jie Chang, <sup>a,b</sup>  
Joey Hui Min Wong, <sup>a</sup> Xian Jun Loh <sup>a,b,c</sup> and Rubayn Goh <sup>a</sup>

Diabetic ocular complications continue to be the leading cause of vision impairment in the world, with a considerable impact to healthcare and the global economy. While there are management strategies currently in place to delay the progression of diabetic ocular disease, risks associated with those strategies still pose a major concern in the clinical field. Management strategies generally involve ocular drug administration and surgical intervention. Some limitations with current ocular drug delivery systems include poor bioavailability of drug formulations and complications arising from drug regimens that require frequent intravitreal injections for drug administration. A vitrectomy is also a common surgical procedure to replace severely damaged vitreous caused by various diabetic ocular complications. However, existing vitreous substitutes used for post-vitrectomy surgery have a certain degree of toxicity to ocular tissues. Thermogels are well-suited materials for the treatment of diabetic ocular diseases as they could mimic the properties of ocular tissues to maintain the viability of therapeutics, serve as drug delivery depots and be tailored to be mechanically robust and non-toxic. Furthermore, the thermoresponsive property of thermogels imparts *in situ* gelling properties to create injectable mediums for minimally invasive disease management strategies. This review covers some of the latest developments in the field, highlighting the advantages of thermogels as sustained drug delivery systems, biocompatible and non-toxic vitreous substitutes, shape conformable implants and long-acting therapeutics over conventional treatments used for the treatment of diabetic ocular diseases.

Received 10th August 2023,  
Accepted 28th September 2023

DOI: 10.1039/d3lp00136a

[rsc.li/rscapplpolym](http://rsc.li/rscapplpolym)

## 1. Introduction

The global epidemic of diabetes is a growing health concern that has been increasingly prevalent over the past few decades. In 2021, approximately 537 million adults worldwide suffer from diabetes with a prevalence of nearly 10.5% among adults aged 20–79. In addition, these alarming statistics are expected to increase to 783 million adults by 2045 with a prevalence of about 12.2%.<sup>1</sup> Diabetes Mellitus is a condition that occurs when the pancreas is unable to produce sufficient insulin, or the body is unable to utilise the insulin produced to break down glucose. This results in hyperglycaemia where glucose levels in the body are elevated and too high.<sup>2</sup> When left

untreated, hyperglycaemia magnifies the risk of developing severe macrovascular and microvascular complications to various tissues and organs. Traditionally, macrovascular complications include stroke, coronary heart disease, and peripheral artery disease, whereas microvascular complications include diabetic kidney disease, peripheral neuropathy, and retinopathy. Emerging evidence has now discovered other complications, such as liver disease, functional and cognitive disability, infections, affective disorders, and sleep disturbances, which were previously not acknowledged to be associated with diabetes.<sup>3</sup> Besides adversely impacting the patient's quality of life, these degenerative complications have incurred a huge health burden on the economy that was worth USD 966 billion in 2021.<sup>1</sup>

Ocular diseases are one of the more frequently incurred comorbidities of diabetes. Hyperglycaemia could induce profound damage to ocular tissues even during the initial stages of the disease.<sup>4</sup> Diabetic retinopathy (DR) is one of the most common manifestations of ocular disease due to diabetes and it is the leading cause of vision loss among adults from Western countries.<sup>5</sup> Other ocular complications of diabetes that could develop and result in vision loss include diabetic macular oedema (DMO), dry eye disease (DED), neurotrophic

*<sup>a</sup>Institute of Materials Research and Engineering (IMRE), Agency for Science, Technology and Research (A\*STAR), 2 Fusionopolis Way, #08-03 Innovis, Singapore 138634, Republic of Singapore. E-mail: rubayn\_goh@imre.a-star.edu.sg, lohxi@imre.a-star.edu.sg*

*<sup>b</sup>Institute of Sustainability for Chemicals, Energy and Environment (ISCE2), Agency for Science, Technology and Research (A\*STAR), 1 Pesek Road, Jurong Island, Singapore 627833, Republic of Singapore*

<sup>c</sup>*School of Materials Science and Engineering, Nanyang Technological University (NTU), Singapore 639798, Republic of Singapore*

† Co-first authors. These authors contributed equally to the work.

keratopathy, cataracts, neovascular glaucoma, and vitreous degeneration or detachment.<sup>5</sup> Despite progress in the medical field, there is currently no cure for hyperglycaemia and its associated ocular complications, only clinical measures to prevent the complications from deteriorating further. Management of blood glucose and blood pressure remains to be the key to reducing the chances of developing most diabetic ocular complications. Regular eye screening has facilitated early diagnosis such that patients receive timely treatment and remain responsive to current treatments.<sup>6</sup> Current pharmacological approaches for hindering the progression of diabetic ocular diseases are mostly steered towards preventing sorbitol accumulation, reducing ocular vascular proliferation, and suppressing adverse inflammatory responses in the eye.<sup>7,8</sup> This would usually be achieved by delivering various therapeutics into specific segments of the eye. Some diabetic ocular disorders such as DED may be addressed by designing biocompatible implants in the form of specialised contact lenses or occlusion plugs to reduce tear loss if the patient does not show improvements with the use of artificial tears or therapeutics used for the management of the disease.<sup>9</sup>

Current routes of therapeutics delivery to ocular tissues vary in their degree of invasiveness for the treatment of ocular diseases. Therapeutics delivery could range from conventional eye drops to direct injection of therapeutics or *via* intravitreal ocular implants for prolonged release in the eye.<sup>10</sup> These traditional routes of delivery have their specific limitations. For instance, therapeutics loaded in eye drops, like anti-glaucoma drugs used for lowering intraocular pressure (IOP), tend to have poor bioavailability due to blink reflex, rapid tear turnover, and poor corneal penetration.<sup>11</sup> Therapeutics delivered *via* intravitreal injections may sometimes cause the development of sight-threatening complications such as endophthalmitis and rhegmatogenous retinal detachment due to poor aseptic and injection techniques.<sup>12</sup> The risk would be further escalated for drugs with

short half-lives in the vitreous humour, requiring frequent intravitreal administrations to maintain the therapeutic effect of the drugs. While intravitreal implants are clinically available to help extend the release of drugs with short half-lives, they are mostly non-biodegradable and would pose similar problems as the need for surgical intervention for its removal exposes patients to possible post-surgical complications.<sup>13</sup> Due to these challenges in effective ocular therapeutic delivery, there is a dire need for novel strategies to advance treatments for diabetic ocular diseases.

In recent years, the use of hydrogels has been identified as an attractive and promising approach for the management of diabetic ocular disease.<sup>14</sup> Among the characteristics of hydrogels that make them versatile are their biocompatibility, mechanical properties that are similar to biological tissues, their micro- and macro-structural integrity, and their ability to determine the local chemical environment. These properties arise from its chemically tailorable three-dimensional networks composed of chemically crosslinked hydrophilic polymer chains that retain large amounts of water while maintaining its structure.<sup>15,16</sup> However, applications of such covalently crosslinked hydrogels have been limited as they require invasive medical procedures and suffer from poor site conformability.<sup>17</sup> As a result, injectability has become an increasingly important criterion as a minimally invasive administration method. This has steered research efforts towards the preparation of hydrogels using non-covalent supramolecular interactions. Examples of these interactions include hydrogen bonding, hydrophobic interactions, ionic interactions, and host-guest bonding.<sup>17,18</sup> These supramolecular interactions are reversible and allow the hydrogel's matrix to be formed and deconstructed under appropriate conditions, for example at certain pH or temperatures.<sup>19</sup> Additionally, the reversibility enables temporary disruption of the hydrogel's matrix, such as during high shear conditions when passing through a needle, before being reformed thereafter.<sup>13</sup>



**Nicholas Wei Xun Ong**

*Nicholas Ong is currently a Ph.D. student at the Department of Materials Science and Engineering, Nanyang Technological University (NTU), Singapore. He is also a research engineer at the Institute of Sustainability for Chemicals, Energy and Environment (ISCE2) at the Agency for Science, Technology and Research (A\*STAR), Singapore. He obtained his BSc in Chemistry and Biological Chemistry from*

*NTU in 2021. His research interests include the development of supramolecular hydrogels and sustainable polymers.*



**Belynn Sim**

*Belynn Sim obtained her BEng in Materials Science and Engineering from Nanyang Technological University (NTU), Singapore. She is currently pursuing a Ph.D. with an A\*STAR Graduate Scholarship at NTU's School of Materials Science and Engineering under the supervision of Prof. Xian Jun Loh and Prof. Xiaodong Chen. Her research interest lies in the field of thermoresponsive hydrogels for biomedical applications.*



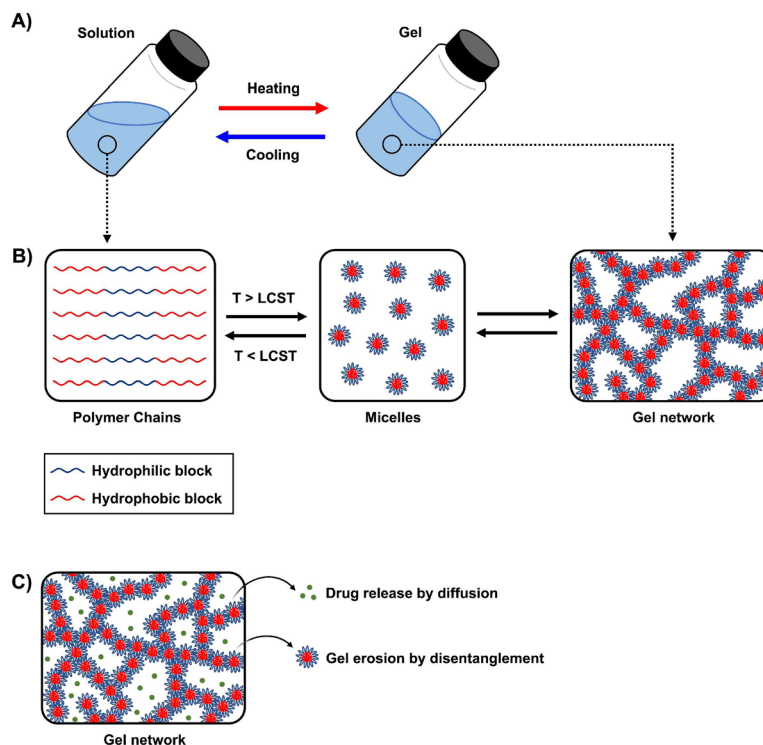


**Fig. 1** Schematic of (A) sol-to-gel transition upon heating, (B) micelle formation and gelation, and (C) drug release and disentanglement of micelles.

## 2. Thermogels for diabetic ocular complications

### 2.1. Properties of thermogels

Thermogels are a subclass of supramolecular hydrogels that exist as free-flowing solutions and undergo sol-to-gel transition at elevated temperatures (Fig. 1A). The automatic transition is driven by hydrophobic interactions forming reversible physical crosslinks, and this unique property is particularly useful as no potentially toxic reagents or crosslinkers are required for gelation.<sup>20,21</sup> Thermogels that are capable of gelation at near

physiological temperature are generally desirable for ocular applications as they could be injected as a solution and promptly form a gel *in situ*.

An important aspect of obtaining thermogels lies in a phenomenon known as the lower critical solution temperature (LCST). Polymers exhibiting LCST contain both hydrophilic and hydrophobic domains and are fully miscible in water below a certain temperature. Above that temperature, the polymer becomes poorly solvated by water molecules around the hydrophobic domains, causing it to undergo a coil-to-globule transition that results in phase separation.<sup>22</sup> It should be noted that this does not mean that the polymer becomes completely hydro-



**Jun Jie Chang**

*Chang Jun Jie obtained his Ph.D. in Chemistry from Nanyang Technological University, Singapore. He is currently a research scientist at the Institute of Sustainability for Chemicals, Energy and Environment (ISCE2), A\*STAR, Singapore. His research focus is on the synthesis of functional polymers and the development of supramolecular hydrogels.*

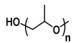
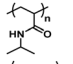
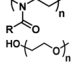
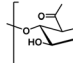
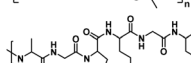
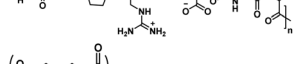
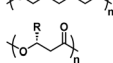
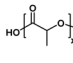



**Joey Hui Min Wong**

*Joey Hui Min Wong received her BEng in Materials Science and Engineering from Nanyang Technological University, Singapore. She is currently a research engineer at the Institute of Materials Research and Engineering (IMRE), A\*STAR, Singapore. Her current research focus is on the development of thermogels for biomedical applications.*



**Table 1** Examples of polymers used in thermogels for ophthalmic applications

| Polymer                              | Structure   | Property  |
|--------------------------------------|---|---|
| Poly(propylene glycol)               |  | Thermoresponsive (LCST: 15–42 °C) <sup>57</sup> |
| Poly( <i>N</i> -isopropylacrylamide) |  | Thermoresponsive (LCST: 32 °C) <sup>58</sup>    |
| Poly(2-oxazoline)                    |  | Thermoresponsive (LCST: 24–97 °C) <sup>59</sup> |
| Poly(ethylene glycol)                |  | Hydrophilic                                     |
| Hyaluronic acid                      |  | Hydrophilic                                     |
| Gelatin                              |  | Hydrophilic                                     |
| Poly(caprolactone)                   |  | Hydrophobic                                     |
| Poly(hydroxybutyrate)                |  | Hydrophobic                                     |
| Poly(lactic-co-glycolic acid)        |  | Hydrophobic                                     |

phobic above the LCST, as the hydrophilic domains remain so even above the LCST.<sup>23</sup> These thermoresponsive polymers are crucial in enabling the preparation of thermogels. Covalently coupling LCST polymers with other water-soluble polymers results in amphiphilic block copolymers that can self-assemble into micelles at elevated temperatures. Poly(*N*-isopropylacrylamide) (PNIPAAm) is perhaps the most studied thermoresponsive polymer for biomedical applications due to its LCST of 32 °C which is close to physiological temperatures.<sup>24,25</sup> Other copolymers exhibiting LCST in aqueous solution such as poly(ethylene glycol) (PEG), poly(propylene glycol) (PPG),<sup>26</sup> and the Poloxamers or Pluronic family of thermoresponsive triblock copolymers (Table 1) are commonly used to prepare thermogels.<sup>27</sup>

Thermogelation can occur *via* micellar aggregation into an ordered three-dimensional network that entraps water

(Fig. 1B), with several models proposed. The Pluronic family is an example of ABA triblock copolymers, where A represents the hydrophilic blocks and B represents the thermoresponsive LCST blocks, that form the gel network *via* spherical micelle packing into a cubic lattice.<sup>28,29</sup> In BAB triblock copolymers, the micelles are proposed to entangle *via* loops and bridges.<sup>30,31</sup> Recent small-angle neutron scattering (SANS) measurements of several BAB block copolymers with varying A and B block lengths showed that these entanglements are highly dependent on the polymer nanostructure interactions and morphology of the micelles.<sup>32</sup> For diblock (AB) micelles having a hydrophilic corona with non-obvious aggregation points, crew-cut or semi-bald micelle models have been put forth.<sup>33–35</sup> More recently, thermogelling polyurethane multi-block copolymers composed of randomly distributed hydro-

**Xian Jun Loh**

*Prof. Xian Jun Loh completed his basic and postgraduate studies at the National University of Singapore. A polymer chemist by training, he is the Executive Director at the Institute of Materials Research and Engineering (IMRE), A\*STAR, Singapore. He is also the current President and member of the Executive Committee of the Singapore National Institute of Chemistry. He is a pioneer in the area of biodegradable thermo-*

*gels, and he is highly knowledgeable in developing materials for various applications including biomedical, engineering, cosmetics, personal care and food.*

**Rubayn Goh**

*Rubayn Goh is a research scientist at the Institute of Materials Research and Engineering (IMRE), A\*STAR, Singapore. He specializes in bioinspired and biomaterials research. He is a recipient of the A\*STAR National Science Scholarship and completed his Ph.D. in Materials from the University of California, Santa Barbara. A materials scientist by training, his research focuses on developing bioinspired self-assembly strategies*

*for nanoarchitected materials and the development of functional capabilities of injectable hydrogels.*





philic and hydrophobic blocks have been developed. They were proposed to form networks *via* the associated micelle model involving “hairy micelles” that associate with each other through the random hydrophobic blocks on the “hairs”.<sup>20,36</sup> The rational design of new thermogelling copolymers can be guided through careful consideration of the gelation mechanism which is influenced by the copolymer architecture and the interactions of its nanostructures.<sup>32,37</sup>

The minimum concentration of polymer in solution before a gel can be obtained is known as the critical gelation concentration (CGC), which can be determined *via* vial-inversion tests, rheological measurements,<sup>38</sup> or dynamic light-scattering.<sup>39</sup> Generally, a polymer having a higher molecular weight with the same composition tends to exhibit lower CGC because of greater entanglements between micelles.<sup>40</sup> Low CGC thermogels are beneficial for their higher water content which improves their biocompatibility.<sup>41</sup> However, one potential consequence of high molecular weight polymers is that they cannot be easily removed from the body. Thermogels targeting the treatment of ocular diseases are typically deposited near the eye, for example inside the vitreous body or in the anterior or posterior chambers. The anterior and posterior chambers are under constant flow of the aqueous humour that drains *via* the trabecular pathway involving the trabecular meshwork and Schlemm's canal.<sup>42</sup> In the case of the vitreous, aqueous flow into the posterior chamber or across retinal pigment epithelium occurs through diffusion or advection.<sup>43,44</sup> Due to bulk or surface erosion of thermogels,<sup>45</sup> the eroded polymer micelles can be carried out of the eye *via* these pathways, eventually ending up in the bloodstream and subsequently removed by the kidneys *via* renal glomerular filtration. The filtration can be impeded or even blocked if the molecular weight of the polymers is too high. For example, poly(ethylene glycol) with molecular weights greater than 10 kDa have significantly reduced rates of renal excretion.<sup>46</sup> To address this issue, biodegradable polymer blocks such as poly(caprolactone) or poly(lactic acid-*co*-glycolic acid) containing hydrolysable ester groups can be inserted into polymer chains to enable their degradation into shorter chains and facilitate their removal from the body.<sup>47–49</sup>

The composition of the polymer chain is also an important parameter affecting the CGC of thermogels. This includes the ratio of hydrophobic to hydrophilic blocks in the polymer, as well as the lengths and molecular weight distributions of the blocks.<sup>50,51</sup> Having a greater composition of hydrophobic macromonomers, such as PPG or poly(lactic-*co*-glycolic acid) (PLGA), lowers the LCST due to increased hydrophobic interactions.<sup>47,52</sup> This initiates micelle self-assembly and subsequent thermogelation at lower temperatures, resulting in lower CGC. Conversely, a greater composition of hydrophilic macromonomers, like PEG, would increase the CGC. Several examples of hydrophobic and hydrophilic polymers, as well as thermoresponsive polymers with LCST that are used in thermogels for ophthalmic applications are shown in Table 1. The polymer's topology has also been found to affect the CGC. Lin *et al.* prepared thermogelling hyperbranched polyurethanes with different degrees of branching.<sup>53–55</sup> They found that the

CGC increases with branching, likely due to reduced polymer entanglements from a more globular geometry.<sup>53</sup> Micellization is an entropically driven process from the dehydration of hydrophobic blocks. An increase in branching resulted in less positive entropic values ( $\Delta S$ ),<sup>54,55</sup> leading to an overall increase in the Gibbs free energy ( $\Delta G$ ) and thus indicated a less exergonic and spontaneous process. Since the gelation temperature and CGC of thermogels are closely intertwined, the gelation temperature can be tuned *via* careful formulation based on the parameters mentioned above.<sup>15,20,52,56</sup>

## 2.2. Applications of thermogels for diabetic ocular disease management

Current research work on thermogels for ocular applications demonstrates the ability of thermogels to be utilized as drug depots for sustained drug delivery, vitreous substitutes, shape-conformable implants such as punctal plugs, and long-acting therapeutics (Fig. 2).

When thermogels are injected into the body, they could function as depots that store therapeutics such as drugs or peptides within its three-dimensional matrix. The solubilization of hydrophobic drugs is particularly facilitated by the hydrophobic blocks of the constituent polymers in the thermogel. Owing to the porous matrix at the molecular scale, encapsulated therapeutics can be released *via* diffusion and erosion of the matrix by gradual disentanglement of the micelles (Fig. 1C). Correspondingly, controlled, sustained, and also localized therapeutic release from the thermogel depot can be achieved for the treatment of diabetic ocular diseases, which is advantageous to conventional methods of drug delivery requiring high dosages and more frequent administration.<sup>60</sup> The thermogel's crosslinking density can influence the porosity of the matrix as well as the strength of micellar interactions, which in turn dictates the duration of therapeutic release. Secondary crosslinking sites which are triggered by the addition of secondary crosslinking agents, metal ions, dynamic covalent bonds, or host-guest interactions can be introduced into the thermogel to increase the crosslinking density.<sup>61–64</sup> A secondary benefit of a thermogel depot with slower drug release kinetics is that it extends the effective duration of drugs with a short half-life. For example, the sustained release of the diabetic drug, liraglutide, with a half-life in the order of hours was able to be maintained over several days *in vitro*.<sup>65</sup> Another factor that influences the release of therapeutics is the presence of non-covalent interactions between the drug and the thermogel. For instance, electrostatic interactions have been shown to influence the release rate of ionic drugs from thermogels with charged polymer backbones.<sup>66</sup> Therefore, the rate of therapeutic release from thermogels can be tuned through rational design.

Besides the favorable drug release capabilities of thermogels for ocular applications, the high water content in thermogels makes them excellent vitreous substitutes or tamponading materials with similar densities and refractive indices.<sup>67</sup> The transparency and stiffness of the gel are important parameters to consider for ocular applications, and a clear and transparent vitreous substitute ensures good optical clarity immediately post-





Fig. 2 Ocular applications of injectable thermogels.

surgery.<sup>68</sup> While the polymer molecular weight and composition can be altered to tune the CGC and gelation temperatures, they have also been found to influence the gel's opacity.<sup>40,69</sup> Moreover, a vitreous tamponade is recommended to have a minimum storage modulus of 100 Pa to withstand the regular fast motion of the eye.<sup>70</sup> Therefore, a balance between the gel storage modulus and its opacity is required to ensure the thermogel's suitability as a vitreous tamponade. Furthermore, since thermogels could be tailored to match the mechanical properties of ocular tissues, the *in situ* thermogelling properties could also be utilized to produce shape-conformable ocular implants.

In the following sections, this review would highlight the development of thermogels over the past few decades for the management of various diabetic ocular complications. The literature examples are summarized in Table 2.

### 3. Types of diabetic ocular complications

#### 3.1. Diabetic retinopathy, macular oedema and neovascular glaucoma

DR is one of the most common microvascular complications of diabetes mellitus and is a major cause of blindness among

the global adult working population.<sup>96,97</sup> DR is characterized as a microvascular neurodegenerative disease where persistent high blood sugar impairs neurovascular cells of the retina causing various neurovascular complications. DR can be divided into two categories: non-proliferative diabetic retinopathy (NPDR) and proliferative diabetic retinopathy (PDR). NPDR occurs when hyperglycemia disrupts the production and regulation of neuroprotective factors causing retinal neurodegeneration, early microvascular impairment, and neurovascular unit impairment. These lead to thickening of the retinal basement membrane, disruption of endothelial tight junctions and retinal pericyte loss, causing blood-retinal barrier dysfunction which results in vascular leakage. As NPDR progresses, chronic and higher severity vascular damage leads to regions of ischemia in the retina due to capillary non-perfusion, causing capillary occlusion and degeneration. PDR occurs when proangiogenic growth factors are produced in response to chronic or worsening ischemia to cause retinal neovascularization.<sup>98,99</sup> The new blood vessels formed *via* retinal neovascularization are structurally weak and tend to grow into the vitreous body. A non-clearing vitreous hemorrhage or the development of tractional retinal detachment from extensive vitreous scarring would lead to severe loss of vision.<sup>98–100</sup> A posterior pars planar vitrectomy would be



**Table 2** Literature examples of thermogels for the management of various diabetic ocular complications

| Drug delivery systems                       |                                 |                          |                           |   |           |
|---|---------------------------------|--------------------------|---------------------------|---|-----------|
| Polymer                                     | Application                     | Payload                  | Administration route      | Delivery performance  | Ref.      |
| PEG-PPG-PCL (EPC)                           | Diabetic retinopathy            | Bevacizumab, Aflibercept | Intravitreal              | Sustained release of bevacizumab and aflibercept for 40 days <i>in vitro</i> . Released anti-VEGFs show functional bioactivity; inhibited HUVEC cell proliferation <i>in vitro</i> , inhibited angiogenesis in rat <i>ex vivo</i> choroidal explants and inhibited VEGF-driven neovascularization in rabbit model   | 71        |
| PEG-PPG-PTHF (EPT)                          | Intraocular drug delivery depot | BSA                      | Intravitreal              | Released 50% of BSA over 28 days <i>in vitro</i> .  | 72        |
| PEG-serinol hexamethylene urethane (ESHU)   | Diabetic retinopathy            | Bevacizumab              | Intravitreal              | Bevacizumab released from ESHU over 16 weeks with minimal burst release <i>in vitro</i> . However, burst release of bevacizumab was observed <i>in vivo</i> , bevacizumab was released from ESHU for up to 9 days. ESHU could deliver and maintain a concentration of bevacizumab in the vitreous that is 4.7 times higher than delivery through bolus injection. | 73        |
| PEOz-PCL-PEOz (ECE)                         | Diabetic retinopathy            | Bevacizumab              | Intravitreal              | Diffusion-controlled release of bevacizumab for 11 days, erosion- and diffusion-controlled release thereafter up to 20 days <i>in vitro</i> .   | 74        |
| PLGA-PEG-PLGA (PPP)                         | Diabetic retinopathy            | Bevacizumab              | Intravitreal              | PPP sustained the release of bevacizumab for 14 days <i>in vitro</i> with 10–13% burst release within the first 8 hours and marginal release thereafter. Avastin®-loaded PPP extended the presence of the protein in the vitreous humour and retina for 4 weeks.  | 75        |
| PLGA/PNIPAAm-PEG                            | Diabetic retinopathy            | Ranibizumab, Aflibercept | Intravitreal              | Ranibizumab or aflibercept could be loaded and released from the thermogel for at least 6 months <i>in vitro</i> . Anti-VEGF agent loaded thermogel could deliver bioactive payload for at least 12 weeks.  | 76–78     |
| PLGA/PEG-PLLA DA                            | Diabetic retinopathy            | Aflibercept              | Intravitreal              | Sustained the release of aflibercept for at least 6 months <i>in vitro</i> . Aflibercept-loaded thermogel could deliver a bioactive payload for at least 6 months.  | 79 and 80 |
| PLGA/PNIPAAm-PEG                            | Neovascular glaucoma            | Brimonidine              | Topical (eye drops)       | Sustained the release of brimonidine and reduced the IOP of rabbit eyes for at least 28 days.   | 81        |
| LDH/PLGA-PEG-PLGA                           | Neovascular glaucoma            | Brimonidine              | Topical (eye drops)       | Sustained the delivery of brimonidine for up to 144 hours <i>in vitro</i> with 75% burst release within first 10 hours and subsequent 15% slow sustained release. Therapeutic levels of brimonidine could be maintained <i>via</i> delivery through the thermogel system in rabbit's cornea for up to 168 hours.  | 82        |
| Chitosan/gelatin/ $\beta$ -glycerophosphate | Neovascular glaucoma            | Latanoprost              | Subconjunctival injection | Sustained the release of 67.72 $\pm$ 4.25% latanoprost over 28 days. <i>In vivo</i> studies carried out on glaucomatous rabbit eyes showed latanoprost-loaded thermogel could reduce intraocular pressure to normal levels within 8 days.   | 83        |
| Hexanoyl glycol chitosan (HGC)              | Neovascular glaucoma            | Brimonidine              | Topical (eye drops)       | Instillation of brimonidine-loaded HGC lowered IOP of rabbit eyes from baseline levels for 14 hours, which is 2-fold longer than conventional anti-glaucoma eye drop formulation Alphagan P.  | 84        |



Table 2 (Contd.)

| Drug delivery systems  |                                 |  |                           |   |      |
|--|---------------------------------|--|---------------------------|---|------|
| Polymer  | Application                     | Payload  | Administration route      | Delivery performance  | Ref. |
| Poly(NIPAAm-co-NAS-co-mDEX)-PEG-poly(NIPAAm-co-NAS-co-mDEX)-cysteamine (PNADEX-CA) | Diabetic retinopathy            | Dexamethasone  | Intravitreal              | Sustained release of native dexamethasone for over 430 days <i>in vitro</i> . Software to simulate <i>in vivo</i> release showed prolonged release of dexamethasone while maintaining therapeutic concentration in the vitreous for at least 500 days.  | 85   |
| Chitosan-gelatin   | Cataracts                       | Levofloxacin   | Topical (eye drops)       | Sustained release for over 7 days <i>in vitro</i> .   | 86   |
| MSN/PLGA-PEG-PLGA  | Cataracts                       | Prednisolone acetate<br>Levofloxacin   | Subconjunctival injection | Prolonged release of PA and short-term release of levofloxacin within 28 days <i>in vitro</i> .   | 87   |
| PLGA/PLCL-PEG-PLCL   | Cataracts                       | Levobunolol<br>Dexamethasone,<br>Moxifloxacin  | —                         | Short-term slow release of moxifloxacin for up to 15 days and even slower prolonged release of dexamethasone and levobunolol for more than a month <i>in vitro</i> .  | 88   |
| mPEG-PLA NLC/plurionics (26% F127/1.5% F68)  | Cataracts                       | Dexamethasone,<br>Moxifloxacin,<br>Genistein   | —                         | Within 10 days, moxifloxacin was completely released <i>in vitro</i> . Dexamethasone experienced a burst release profile in the first week, followed by a sustained release for 30 days. Genistein gradually released at a decreasing rate till day 40. Inhibited proliferation, migration and epithelial-mesenchymal transition of lens epithelial cells (SRA 01/04) in a dose-dependent manner. | 89   |
| Gelatin-PNIPAAm-helix pomatia agglutinin   | Dry eye disease                 | Epigallocatechin gallate (EGCG)  | Topical (eye drops)       | Sustained release of EGCG for over 14 days <i>in vitro</i> .  | 90   |
| MPOSS-PEG-PPG  | Dry eye disease                 | FK506  | Topical (eye drops)       | Prolonged release of FK506 for over 20 days.  | 91   |
| Chitosan/poloxamer (C/P407)  | Dry eye disease                 | Insulin  | Topical (eye drops)       | Slow release of insulin over 15 days.   | 92   |
| Tamponade material/ocular implant  |                                 |  |                           |   |      |
| Polymer  | Application                     | Performance  |                           |   | Ref. |
| PEG-PPG-PCL (EPC)  | Endotamponade                   | EPC maintained in the vitreous for at least 1 year. Induced vitreous regeneration and inhibited retinal scarring post-vitreectomy  |                           |   | 93   |
| PEG-PPG-PCL-Glycerol (EPCG)  | Endotamponade                   | EPCG supported the eye as a vitreous tamponade in rabbit eye models and naturally biodegraded and cleared out of vitreous after 4 months.  |                           |   | 53   |
| PHBHx-PEG-PPG (PHxEP)  | Endotamponade                   | PHxEP supported retinal structure as an endotamponade in rabbit eyes over 180 days, maintaining normal IOP.  |                           |   | 69   |
| Hydroxybutyl chitosan (HBC)  | Punctal plug (dry eye disease)  | HBC punctal plugs reduced tears flow flux by 76.9% and the plug persisted for over 4 weeks post-implantation.  |                           |   | 94   |
| Sulfated HA-PNIPAAm  | Long-acting therapeutic implant | <i>In vivo</i> studies using rabbit dry eye models with a one-time topical application of the thermogel demonstrated ~99% repair of corneal epithelial defects, prevention of cellular apoptosis with ~68.3% cells recovered, and suppression of ocular surface inflammation by 4 folds within 7 days. |                           |   | 95   |

required to remove a portion of the vitreous body and replace the resected vitreous with a vitreous tamponade. DMO may also occur at any level of DR when the extravasation of fluids due to vascular damage occurs at the macular region to cause swelling and blurry vision.<sup>98,99</sup> Neovascular glaucoma may also develop in patients with long-term PDR due to chronic retinal ischemia causing angiogenic factors to diffuse to the anterior segment of the eye. This diffusion could also sometimes be induced for diabetic patients receiving a vitrectomy or lensectomy as well.<sup>100,101</sup>

Treatments are available to manage various complications that arise from DR. Panretinal laser photocoagulation (PRP) is the standard technique used for the treatment of PDR and other vascular angiogenic abnormalities. It involves using a laser to burn and seal abnormal or leaking blood vessels and destroy ischemic retina tissues. A reduction in the area of ischemic retinal tissues helps alleviate hypoxia and encourages the regression of retinal neovascularization.<sup>98,102</sup> However, various adverse side effects may occur with PRP and they range from complications such as a decrease in peripheral and





Therefore, intravitreal injection is currently the best route for the administration of therapeutics to the posterior segment of the eye. Intraocular implants that could extend the release of therapeutics were thus developed to reduce the frequency of intravitreal injection required for treatment. Some examples of clinically approved implants are Illuvein®<sup>113</sup> and Ozurdex®<sup>114</sup> used for sustained intraocular steroid delivery and Susvimo™ which uses a port delivery system for the delivery of anti-VEGF agent, ranibizumab.<sup>115</sup> However, there is a risk with intraocular implants that may cause patients to develop various sight-threatening complications.<sup>116,117</sup> This has led to the continued pursuit of other novel delivery systems that could serve as a universal depot for prolonged ocular drug delivery.

The diagram illustrates the barriers to drug delivery in the eye. It shows a cross-section of the eye with various layers and structures labeled. The tear film is shown on the surface, consisting of a lipid layer, aqueous layer, and mucous layer. The corneal barrier is shown below the tear film, consisting of the epithelium, Bowman's layer, stroma, Descemet's membrane, and endothelium. The eye is divided into the anterior segment and the posterior segment by a dashed line. The anterior segment contains the aqueous humor, and the posterior segment contains the vitreous. The blood aqueous barrier is located at the iris, and the blood retinal barrier is located at the retina. The diagram also shows the administration of a topical eye drop and an intravitreal injection.

© 2023 The Author(s). Published by the Royal Society of Chemistry

peutics<sup>60</sup> and its composition can be tuned to gel at physiological vitreous temperature (35 °C), various thermogelling polymers have been explored for the release of therapeutics to manage DR and its associated complications.

Generally, conventional block copolymer thermogels could entrap therapeutic molecules in its micelle networks to extend the release of various therapeutic agents such as anti-VEGF agents, anti-glaucoma drugs, and intraocular steroids.

A multiblock copolymer thermogel was designed by Xue *et al.* for the release of anti-VEGFs like bevacizumab and aflibercept.<sup>71</sup> This thermoresponsive copolymer (termed as EPC) was a biodegradable polyurethane consisting of PEG, PPG, and hydrolysable polycaprolactone (PCL) segments coupled with 1,6-hexamethylene diisocyanate (HMDI). The authors studied the release of aflibercept from EPC thermogels containing different PEG:PPG ratios from 1:1 to 6:1 and found that slower release was obtained at higher PEG to PPG ratios. Confocal imaging of fluorescein-conjugated rabbit IgG-loaded thermogels stained with Nile Red dye (Fig. 4) revealed that the IgG protein domain sizes were dependent on the PEG and PPG ratios. EPC thermogels consisting of lower PEG to PPG ratios (1:1, 2:1) showed hydrophilic protein domains (in green) that

were larger while gels with higher PEG to PPG ratios (4:1, 6:1) had smaller but more homogeneous protein domains. The results were attributed to the hydrophilic proteins having lesser partitioning away from the hydrophobic polymer phase in the more hydrophilic EPC thermogels (4:1, 6:1) that allowed for more interaction between the polymer matrix and the loaded protein drug which led to slower rates of release of hydrophilic anti-VEGFs. The thermogel formulation with a PEG to PPG ratio of 4:1 was able to sustain the release of bevacizumab and aflibercept for 40 days *in vitro* and the released anti-VEGFs were found to remain bioactive based on Human Umbilical Vein Endothelial Cells (HUVEC) proliferation assay, *ex vivo* model of choroidal sprouting and *in vivo* on rabbit models with persistent retinal neovascularization. From *in vivo* experiments, intravitreal injection of EPC thermogels at a PEG:PPG ratio of 4:1 loaded with aflibercept could suppress ocular angiogenesis for at least 28 days.<sup>71</sup>

Zhang *et al.* subsequently modified EPC by substituting PCL with poly(tetrahydrofuran carbonate) diol (PTHF) to obtain a thermogel (termed as EPT).<sup>72</sup> PTHF was used because it is structurally similar to PEG and PPG and it is a material that has been previously used for long-term biomedical appli-



**Fig. 4** Confocal laser scanning microscopy showing protein distribution within thermogel. (A) Confocal laser scanning microscopy images of stained protein loaded in 20 wt% EPC thermogel. (B) Confocal laser scanning microscopy images coloured according to size where small, medium, and large domains are orange, green and purple respectively. (C) Quantification of total average size of fluorescent domains for EPC with different PEG/PPG ratios. (D) Quantification of average size of medium and large domains ( $n = 3$ ) (\* $p < 0.05$ ; \*\* $p < 0.01$ ; \*\*\* $p < 0.005$ ). Reproduced from ref. 71 with permission from the Royal Society of Chemistry 2019.

cations due to its high stability and biocompatibility<sup>118</sup> and its ability to modulate the gelation temperature of other thermogel systems.<sup>119</sup> The PEG:PPG ratio of 4:1 was maintained while the amount of PTHF was varied. The optimized EPT composition containing 5.7% PTHF by weight yielded the best properties for extended intraocular drug delivery applications. This composition of EPT was able to resist structural erosion better than EPC while still maintaining its ability to biodegrade and be naturally cleared from the vitreous of the eye. This was demonstrated when it was found that EPC degrades completely and becomes undetectable in the vitreous at 3 months post-implantation while about 30% of EPT would still be observable for the same duration. Release kinetic studies performed *in vitro* with Bovine Serum Albumin (BSA) as a model drug showed that EPT had a consistent protein release profile and was able to release 50% of the loaded amount over 28 days *in vitro*, which indicates its ability for extended protein release<sup>72</sup> and the potential for long-term anti-VEGFs delivery for the treatment of DR.

Another multiblock polyurethane thermogel was fabricated by Park and co-workers consisting of Poly(*N*-Boc-serinol) as the hydrophobic block and PEG as the hydrophilic block for the delivery of the anti-VEGF agent, bevacizumab.<sup>73</sup> This biodegradable PEG-poly-(serinol hexamethylene urethane) (ESHU) thermoresponsive hydrogel could be injected at 15 wt% polymer in PBS solution or a solution of bevacizumab in its sol state and undergo a rapid sol-gel phase transition at 37 °C. This thermogel is also well tolerated and biocompatible as it was shown that ESHU does not cause toxicity or adverse effects to corneal endothelial cells nor does it affect retinal function. The authors subsequently demonstrated that ESHU is capable of sustaining the release of bevacizumab for 16 weeks with minimal burst release *in vitro*.<sup>73</sup> However, a burst release was observed when bevacizumab-loaded ESHU was delivered *via* intravitreal injection into rabbit eyes with a subsequent sustained release for up to 9 weeks. Nonetheless, ESHU could support and maintain a bevacizumab concentration that was 4.7 times higher than eyes receiving bevacizumab delivered *via* bolus injection.<sup>120</sup>

Wang *et al.* designed a tri-block poly(2-ethyl-2-oxazoline)-PCL-poly(2-ethyl-2-oxazoline) (PEOz-PCL-PEOz) copolymer thermogelling polyurethane (termed as ECE) for sustained intraocular release of bevacizumab.<sup>74</sup> This copolymer is composed of an amphiphilic (PEOz) block and a PCL biodegradable hydrophobic block coupled together by HMDI. The authors demonstrated the ability of ECE copolymer to load a solution of bevacizumab at low temperatures and undergo sol-to-gel transition in response to elevated temperatures at 37 °C. *In vitro* release studies were carried out by incubating a bevacizumab-loaded ECE polymeric solution in an ocular saline solution at 37 °C. Samples of the released bevacizumab were quantified *via* enzyme-linked immunosorbent assay (ELISA). The study showed a diffusion-controlled release of 40 µg day<sup>-1</sup> for the first 11 days and a combination of erosion- and diffusion-controlled release for day 11–20. Erosion-controlled release was confirmed by scanning electron microscopy (SEM) to

observe changes to hydrogel morphology. At day 20, 80% of the loaded bevacizumab was released and was tested biologically active. Intravitreal injection of ECE into rabbit eyes showed that the rabbit could preserve its normal neuroretinal functions for two months. This demonstrates the safety and effectiveness of the thermogel system.<sup>74</sup>

Another tri-block PLGA-PEG-PLGA (PPP) thermogelling copolymer was reported by Xie *et al.* for the sustained release of bevacizumab (Avastin®) to treat posterior segment angiogenic vascular disorders.<sup>75</sup> PEG is the hydrophilic component and PLGA is used as the hydrophobic and thermoresponsive component to form the thermogelling polymer. Based on rheological studies, PPP with a PEG:PLGA weight ratio of 1:2.6 has a sol-gel transition temperature of 26 °C at 20 wt%. However, when bevacizumab was loaded into PPP, the gelation temperature lowered to between 22–24 °C, depending on the concentration of the protein. The authors suggested that hydrophobic interaction between bevacizumab and hydrophobic segments of PPP results in a lower gelation temperature. This hydrophobic interaction may also cause undesired protein unfolding which may result in loss of biological activity in the vitreous. Subsequent *in vitro* release studies showed PPP was able to carry out sustained release of bevacizumab over 14 days, with 10–13% burst release within the first 8 hours and marginal release thereafter with no apparent toxicity to the retina. It was also observed through *in vivo* pharmacokinetics studies with rat eyes that PPP could extend the presence of Avastin® in the vitreous humor and retina for 4 weeks (35 ± 14 ng ml<sup>-1</sup>) compared to the absence of Avastin® after 4 weeks *via* direct intravitreal injection. It was however not determined whether the released Avastin® in the vitreous was bioactive.<sup>75</sup>

Besides entrapping therapeutics within the thermogel micelles networks for release, other strategies were also employed to delay the release of therapeutics from thermogels.

A microsphere-thermogel drug delivery system was fabricated by Osswald *et al.* to prolong the release of bioactive aflibercept for ocular delivery. The team first experimented with suspending PLGA microspheres loaded with aflibercept in a PNIPAAm-PEG diacrylate thermogel. This PNIPAAm-PEG diacrylate thermogel with PLGA microspheres drug delivery system (DDS) could be injected at room temperature through a 28-G needle which then transitioned to an opaque gel at physiological temperature for sustained release of anti-VEGF agents. *In vitro* drug release studies in PBS at 37 °C demonstrated that it could extend the release of anti-VEGF agents, ranibizumab and aflibercept, for at least 6 months with minimal toxicity or adverse effects to retinal function based on tests with RPE cells. An initial burst release before a subsequent slow zero-order release of the anti-VEGF agent was observed. Only 47% of the loaded anti-VEGF agent was released after 6 months. A 12-week study on the therapeutic efficiency of the DDS on murine eye models showed that anti-VEGF agents released were bioactive and able to reduce laser-induced neovascular lesions areas by 60% and could successfully further extend the presence of anti-VEGFs in the eye as compared to bolus injection of anti-VEGF agent.<sup>76–78</sup>





The PNIPAAm-PEG diacrylate/PLGA microsphere DDS mentioned previously was non-biodegradable in the body and the release of its payload was largely incomplete. Liu and co-workers subsequently fabricated a degradable DDS made of PEG-co-(L-lactic acid) (PEG-PLLA) diacrylate/NIPAAm that was polymerized *via* free radical polymerization to produce a thermogel that improves the release of more aflibercept loaded PLGA microspheres within the same drug release time frame (Fig. 5).<sup>79</sup> The incorporation of PLLA provided hydrolyzable groups to the copolymer for biodegradation and the thermogel achieved a greater release of aflibercept after 6 months (~66%). The DDS and its degradation byproducts were found to be non-cytotoxic but the bioactivity of aflibercept was found to be lower due to the acidic nature of the degradation byproducts from the PLGA microspheres and PEG-PLLA-DA cross-linked polymer. This was managed by adding basic additives like  $\text{Mg}(\text{OH})_2$  as a neutralizing agent to maintain the bioactivity of aflibercept. Further *in vivo* studies on this degradable DDS showed that aflibercept released was effective at reducing the size of laser-induced neovascular lesions in rat eyes (Fig. 6) without signs of inflammation or ocular abnormalities affecting the eye after 6 months.<sup>80</sup>

Similarly, the hydrophilic anti-glaucoma drug brimonidine could also be encapsulated in PLGA microspheres and dispersed in another PNIPAAm-PEG thermogel for extended-release. Fedorchak *et al.* used a microsphere-thermogel system similar to the one reported by Osswald *et al.* to make an eye drop formulation.<sup>81</sup> The drug delivery system was administered at the lower fornix of rabbit eyes and the release was monitored by measuring IOP over time. This brimonidine-loaded microsphere-thermogel system was able to successfully reduce the IOP of rabbit eyes for at least 28 days. Cytotoxicity tests with conjunctival epithelial cells showed approximately 70% cell viability, which is the minimum acceptable threshold for ocular toxicity according to GHS classification.

A different composite nanoparticle-thermogel system was fabricated by Sun *et al.* where a brimonidine-loaded layered double hydroxide (LDH) nanoparticle formed from  $\text{MgCl}_2$  and  $\text{AlCl}_3$  was dispersed in a PLGA-PEG-PLGA thermogel.<sup>82</sup> Rheological studies and light transmission studies showed

that the composites could spontaneously gel around 37 °C and yielded gels that were mostly transparent with a light transmittance of 56–88% in the visible light range. Brimonidine was released through a dual-control strategy where the release first occurs due to anionic exchange from LDH nanoparticles followed by the diffusion out of the thermogel matrix to the tear film (Fig. 7). The *in vitro* drug release profile of the thermogel composite showed an initial burst release of 75% of loaded brimonidine in the first 10 hours, followed by a sustained release of 15% loaded brimonidine in the next 2 days and slow release for up to 144 hours. *In vivo* studies were carried out on male rabbit eyes where the thermogel composite would be dropped onto the rabbit's cornea before an external contact lens was applied to cover the formulation (Fig. 8). Results of the *in vivo* experiments showed that the thermogel composite had good biocompatibility and was not cytotoxic. Delivery of brimonidine was maintained at therapeutic levels for up to 168 hours which effectively relieves IOP for longer as compared to commercial eye drops such as Alphagan® which only sustains release for up to 48 hours.

Cheng *et al.* developed a thermosensitive polymer blend consisting of chitosan/gelatin/ $\beta$ -glycerophosphate (C/G/GP) as a sustained drug delivery system for Latanoprost, an anti-glaucoma drug used for reducing IOP (Fig. 9).<sup>83</sup> GP is a negatively charged weak base that could neutralize the positively charged groups of chitosan. This decreases electrostatic repulsion while allowing hydrogen bonding and hydrophobic interactions to dominate between polymer chains to impart thermoresponsive properties.<sup>121–123</sup> The C/G/GP polymer blend was reported to be injectable in its solution form, gels at 37 °C and showed good *in vitro* and *in vivo* biocompatibility. The *in vitro* release studies showed that  $67.72 \pm 4.25\%$  of latanoprost was released in PBS from the C/G/GP polymer over 28 days demonstrating sustained release. Further *in vivo* studies done on glaucomatous rabbit eyes showed intravitreal delivery of latanoprost-loaded (C/G/GP) polymer blend could decrease ocular hypertension within 8 days to normal IOP.<sup>83</sup>

Cho *et al.* synthesized hexanoyl glycol chitosan (HGC) through *N*-hexanoylation of glycol chitosan with hexanoic anhydride to form a thermoresponsive hydrogel for sustained delivery of

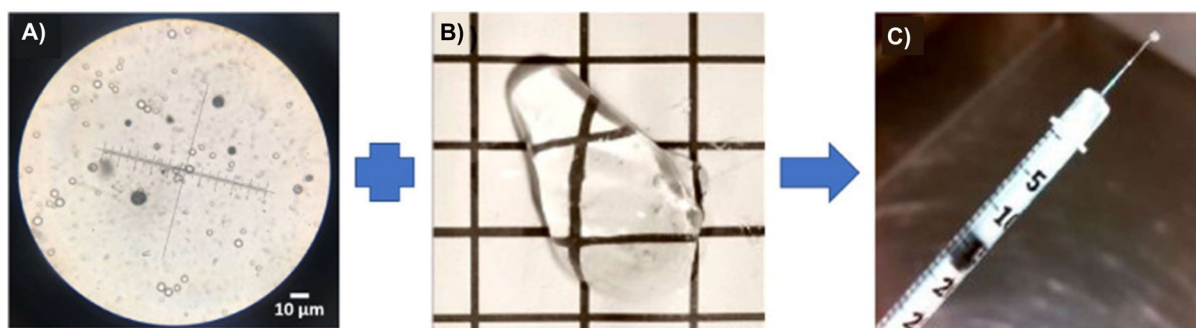


**Fig. 5** Microsphere-thermogel DDS. (A) Aflibercept-loaded PLGA microspheres under a microscope. (B) Blank thermoresponsive PEG-PLLA-DA/NIPAAm thermogel at room temperature. (C) Aflibercept-loaded microsphere-thermogel DDS loaded into a syringe at room temperature. Reprinted from ref. 80, used under Creative Commons CC-BY-NC-ND 4.0 license 2020.





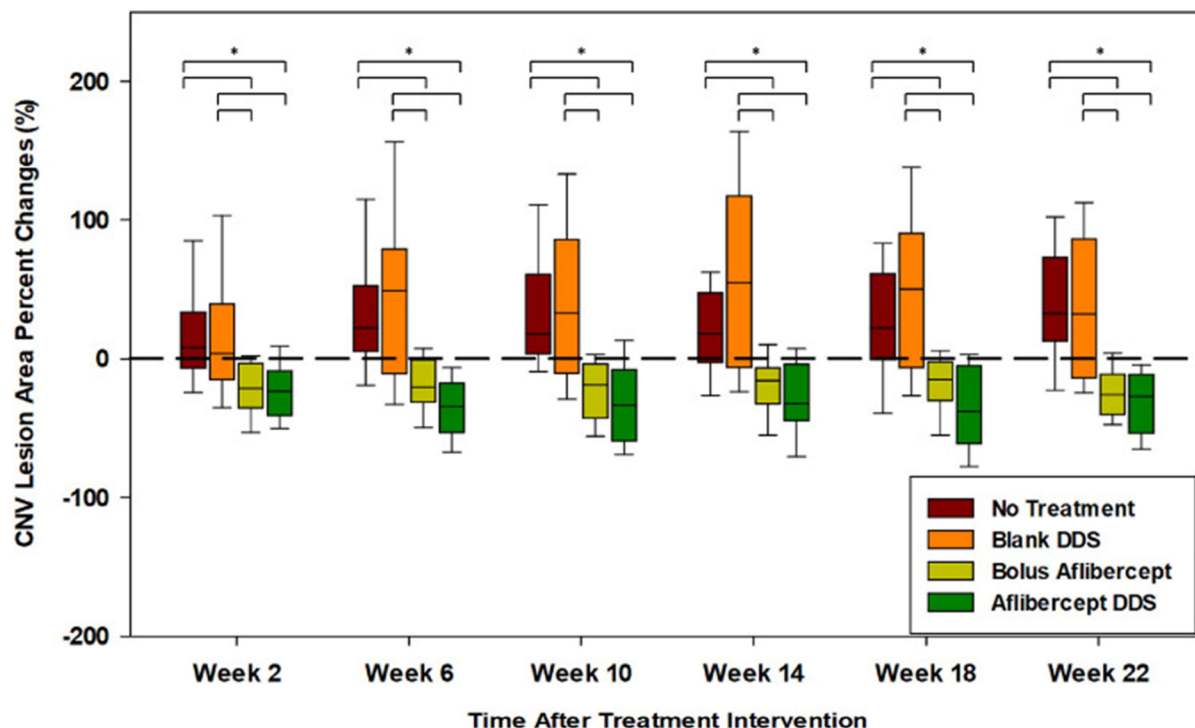


**Fig. 6** Choroidal neovascular lesions (CNV lesions) increase over time for untreated eyes and eyes with blank drug delivery systems. Reduction of choroidal neovascular lesions with aflibercept-loaded DDS was consistently better than routine intravitreal bolus injection of aflibercept throughout the study. Reprinted from ref. 80, used under Creative Commons CC-BY-NC-ND 4.0 license 2020.

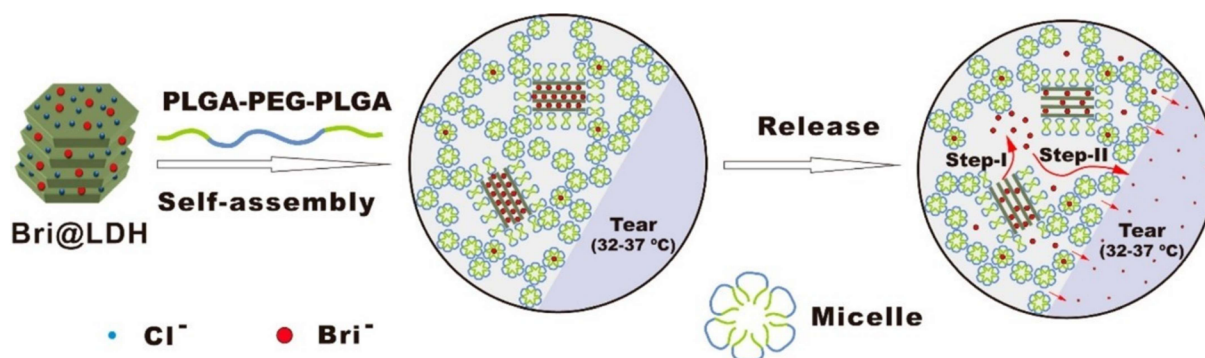


**Fig. 7** Self-assembly of DDS into hydrogels at physiological temperature and the 2-step mechanism involved in the release of brimonidine into the tear film (Step 1: Anionic exchange, Step 2: Diffusion of brimonidine through thermogel matrix). Reprinted with permission from ref. 82. Copyright 2017 American Chemical Society.

brimonidine tartrate for lowering IOP.<sup>84</sup> The hexanoyl groups could self-assemble *via* hydrophobic association to form physical cross-links with increasing temperature (Fig. 10). The gelation kinetics of HGC were modified by increasing the degree of hexanoylation and controlling the concentration of HGC. HGC at 1.25 wt% with  $39.5 \pm 0.4$  degree of hexanoylation could thermogel at 37 °C and demonstrated good biocompatibility *in vitro*. *In vivo* testing with rabbit eye models showed good precocular retention and an extended period of lowered IOP for 14 hours after instillation which was longer than brimonidine tartrate eye drops which lasted 6 hours.

Annala *et al.* fabricated a unique ABA triblock thermosensitive hydrogel made of PEG with its hydroxyl chain ends modified with a chain transfer agent for copolymerization with NIPAM, acrylic acid *N*-hydroxy succinimide ester (NAS), and methacrylated dexamethasone *via* RAFT polymerization.<sup>85</sup> The formed hydrogel could be injected into the vitreous body and subsequently slowly release intraocular steroid dexamethasone *via* hydrolysis of the ester bonds between dexamethasone and the PNIPAm-PEG copolymer chain for delivery to treat ocular inflammatory diseases like DR and DMO. Variation in NIPAM composition modulated the gelation kinetics, while NAS was





**Fig. 8** Diagram demonstrating the application of nanoparticle-thermogel system with contact lens as cover to improve the spread of the drug delivery system. Red dots represent brimonidine releasing into the anterior chamber through the cornea. Reprinted with permission from ref. 82. Copyright 2017 American Chemical Society.

incorporated for reaction with cysteamine to incorporate reversible covalent cross-linking between PNIPAAm-PEG chains of the polymer *via* the formation of disulfide bonds which imparted self-healing and shear thinning properties to the polymer for injectability. The complete copolymer denoted as poly(NIPAAm-*co*-NAS-*co*-mDEX)-PEG-poly(NIPAAm-*co*-NAS-*co*-mDEX)-cysteamine (PNADEX-CA) at 10 wt% was injectable through a 30-G needle with thermal gelation occurring at 37 °C and passed cytotoxicity and biocompatibility tests. Through *in vitro* drug release studies, first-order kinetics release of native dexamethasone was observed in an aqueous medium at pH 7.4 for over 430 days at 37 °C with minimal toxic degradation products. The authors utilized software simulations to demonstrate that an intravitreal administration of 100 mg of 10 wt% PNADEX-CA ( $\sim 623 \pm 32$  ng of dexamethasone) could maintain the therapeutic range of dexamethasone in the vitreous for at least 500 days. While further *in vivo* testing would be required to test the safety and the release kinetics in the vitreous, the design and concept of the thermogelling polymer could potentially be used for delivering other therapeutics of similar nature *via* methacrylate functionalization for the treatment of various ocular diseases.



**Fig. 9** Formation of thermogel via quaternization of chitosan and gelatin and allowing hydrophobic interaction and hydrogen bonding to dominate and induce gelation with increasing temperature. Reprinted with permission from ref. 83. Copyright 2014 Elsevier.

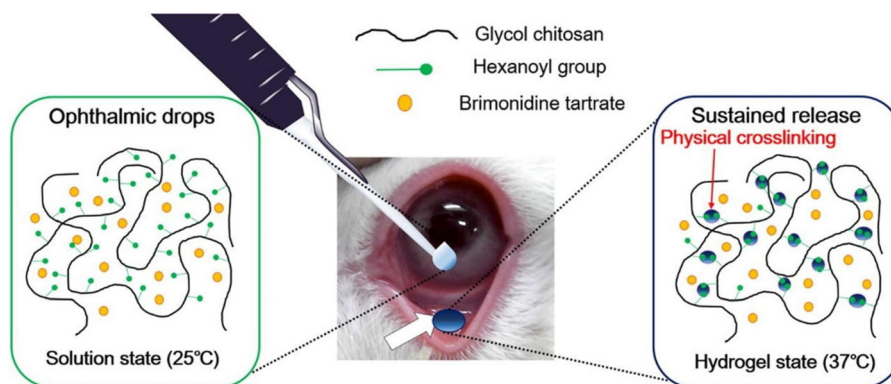


**Fig. 10** Thermogelation of HGC thermogel due to physical crosslinking mediated by hydrophobic association between the hexanoyl group at 37 °C. Reprinted with permission from ref. 84. Copyright 2016 Elsevier.



### 3.3. Vitreous substitutes for post-vitrectomy surgery

Diabetic patients with tractional retinal detachment or severe vitreous haemorrhage from PDR are treated by performing a vitrectomy to replace the vitreous body of the retina with a vitreous substitute. The substitute needs to promote retina re-adhesion to the retinal pigment epithelium and serve as a tamponade agent. At present, clinically available vitreous substitutes include liquids (silicone oil, perfluorocarbon liquids (PFCL), semi-fluorinated alkanes) or gases (air, SF<sub>6</sub>, C<sub>2</sub>F<sub>6</sub>).<sup>124</sup> Gaseous substitutes tend to have a low residence time in the vitreous body and are more often used for intraoperative procedures that require a temporary tamponade. It also requires patients to remain face down for an extended duration post-operation for the tamponade to work on the retina. Liquid substitutes like PFCL have good tamponading properties but are toxic to ocular tissues and cells when it is left in the vitreous for extended periods of time. They are usually replaced with silicone oil after a few months, which may induce further trauma to the eye during the removal and re-application of the new vitreous substitute. Nonetheless, silicone oil and semi-fluorinated alkanes would also require removal from the vitreous cavity as they would eventually undergo emulsification to cause retinal inflammation and the development of cataracts and other complications that could affect visual acuity.<sup>124</sup> Therefore, there is a need to explore alternative materials that are safe and could last longer than current vitreous substitutes in the market.<sup>68,124,125</sup> Therefore, there is a need to explore alternative materials that are safe and could last longer than current vitreous substitutes in the market.<sup>68,125</sup>

As the native vitreous mostly consists of collagen and hyaluronic acid and has viscoelastic properties that resemble hydrogels, various natural and synthetic hydrogels have been investigated to develop medium to long-term vitreous tamponades.<sup>67,68</sup> Hydrogels derived from natural biopolymers tend to have very short residence time and suffer from batch-to-batch variations which makes them unreliable for clinical use.<sup>124</sup> Chemically cross-linked synthetic hydrogels are also not suitable for ocular applications as the monomers used are toxic to ocular tissues and would usually fragment after being injected through a small-bore needle, ruining its hydrogel properties. Current research efforts have focused on robust *in situ* physically cross-linked hydrogels that can be injected as a liquid followed by gelation in response to a physical stimulus, and which intrinsically possess enough surface tension and elasticity to provide a long-lasting tamponading force to support the retina and seal tears post vitrectomy.<sup>124,126</sup> Several biocompatible thermogels have been reported that meet the criteria for use as a vitreous tamponade material and would be as described below.

### 3.4. Thermogels as vitreous substitutes

The multiblock copolymer polyurethane thermogel consisting of PEG, PPG, and PCL (termed EPC) was fabricated by Liu *et al.* and the thermogel formed could also serve as a vitreous tamponade.<sup>93</sup> It could be injected through a 23-G needle in its

sol state while maintaining its viscosity and surface tension after forming a gel when administered into the vitreous cavity. This is paramount as a vitreous tamponade needs to bridge the retinal break and reappose the detached retina with enough surface tension through swelling counter-force exertion.<sup>67</sup> The optimal polymer concentration of the EPC thermogel was found to be 7 wt%, which yielded an optically clear gel with a refractive index similar to the natural vitreous. It was also determined to be a good long-term vitreous substitute, remaining in the eye even one year after application. EPC also supported vitreous regeneration *in vivo* without requiring cells or drugs to promote the regeneration process. Proteomic analysis showed that the regenerated vitreous-like body was similar in composition to the natural vitreous (924 out of 1177 natural vitreous proteins identified). This surprising finding contradicts the traditional consensus that the vitreous is unable to reform after vitrectomy and could pave the way in directing how future hydrogels could be designed as vitreous substitutes.<sup>93</sup> A recent study on the EPC thermogel also showed inhibited retinal scarring post vitrectomy in an *in vivo* experimental proliferative vitreoretinopathy rabbit model and *in vitro* induced RPE contraction models.<sup>67,127</sup>

EPC thermogels that were lower in molecular weight ( $M_n$  25 kDa) were mechanically weak and caused retinal toxicity after 3 months of implantation in rabbit eyes. The ideal molecular weight range of the copolymers was found to be between 40 to 50 kDa. While higher molecular weight EPC ( $M_n$  ~75 kDa) are mechanically stronger, they were also found to be optically opaque upon gelation due to higher hydrophobic aggregation and the formation of light scattering points. A hyper-branched EPC-Glycerol (EPCG) was thus fabricated to limit intermolecular interaction during self-assembly of the polymeric chains to improve opacity at higher molecular weights.<sup>53</sup> Glycerol was incorporated to impart random primary and secondary branches in the copolymer. EPCG with a glycerol concentration of 0.25 wt% similarly formed thermogels at 7 wt% like the linear, lower molecular weight EPCs and could also maintain optical transparency. *In vivo* studies carried out on rabbit eye models showed that the hyper-branched gel served as a suitable vitreous tamponade that could naturally biodegrade and clear out of the vitreous after 4 months.

The EPC thermogel was also modified by changing the polycaprolactone block to a poly[(*R*)-3-hydroxybutyrate-(*R*)-3-hydroxyhexanoate] (PHBHx) to form an optically clearer thermogel. Xue *et al.* fabricated a poly(PHBHx-PEG-PPG urethane) (PHxEP) thermogel,<sup>69</sup> where the optical transparency was measured with changes to PHBHx ratio. At low concentrations (0.5 wt%), PHxEP had more than 90% transmittance at 37 °C to 500–600 nm wavelengths. Increasing PHBHx concentrations (2, 5, 8 wt%) yielded cloudy gels with transmittance levels lower than 5%. This PHxEP thermogel had sufficient mechanical strength to serve as a vitreous substitute like EPC and was also biocompatible. *In vivo* studies using rabbit eyes demonstrated its ability to retain retinal structure as an endotamponade over a 180-day period while imparting normal IOP.





### 3.5. Cataract from diabetes mellitus

Cataract is an ocular complication that could develop during the early stages of diabetes. Numerous studies have shown that diabetic patients are predisposed to five times increased risk of developing cataracts.<sup>128</sup> The pathogenesis of diabetic cataracts can be ascribed to three main pathways: the polyol pathway, oxidative stress, and the non-enzymatic glycation of lens proteins.<sup>129,130</sup> Within the lens, glucose is converted to sorbitol by the enzyme aldose reductase *via* the polyol pathway. Consequently, hyperglycaemia triggers an overproduction of sorbitol, which accumulates intracellularly and induces a hyperosmotic effect. This results in hydropic swelling of lens fibres that degenerate and form cataracts.<sup>128,131</sup> Moreover, oxidative stress contributed by excessive generation of reactive oxygen species in the eye of diabetic patients causes oxidative damage to lens fibre cells.<sup>128,132</sup> Lastly, elevated glucose levels within the aqueous humour induce non-enzymatic glycation of lens proteins. This results in excessive generation of advanced glycation end products, which form protein aggregates that precipitate in the lens and cause opacity.<sup>128,133</sup>

A cataract is treated with cataract surgery where the cataractous lens is extracted and replaced by an intraocular lens implant. Modern cataract removal techniques involve phacemulsification to reduce the incidence of complications acquired from the surgical procedure.<sup>87</sup> Despite this, serious post-surgical side effects such as endophthalmitis, inflammation, or posterior capsule opacification (PCO) may still develop.<sup>134</sup> As a precautionary measure, antibiotic ophthalmic drops must be routinely applied for a week to prevent bacterial infections and corticosteroids are consistently applied for a month to suppress inflammation.<sup>135,136</sup> However, post-operative care with ophthalmic drops tends to be ineffective due to the low bioavailability of eyedrops, poor patient compliance, and poor eye drop administration technique.<sup>137</sup> Furthermore, the only effective treatment currently available for PCO is laser capsulotomy, and the procedure exposes patients to post-laser complications. There are no clinically approved eye drops available for the treatment of PCO.<sup>89</sup> Recent studies have unveiled that thermogels can potentially serve as an alternative drug delivery medium for multiple therapeutic molecules to provide effective long-term drug release to the eye by injection into the anterior chamber of the eye after cataract surgery.<sup>137</sup>

### 3.6. Thermogels for post-cataract surgery management

Cheng *et al.* formulated a thermoresponsive chitosan-gelatin-based hydrogel loaded with a broad-spectrum antibiotic, levofloxacin.<sup>86</sup> Results showed that the formulation undergo sol-gel transition at 34 °C to form a gel film with an osmolality of 304 mOsm L<sup>-1</sup> within 81.73 s. Drug release studies demonstrated sustained release of levofloxacin from the thermogel for over 7 days. Anti-bacterial studies revealed that sustained release of levofloxacin effectively inhibited the growth of two common pathogens responsible for post-operative endophthalmitis, *S. aureus*, and *S. epidermidis*, for at least 7 days. These results indicate that the levofloxacin-loaded thermogel could

be applied to ocular surfaces after cataract surgery to provide antibiotic effects which eliminates the need for intracameral injections or topical drop application of antibiotics and their associated risks.

Besides administering antibiotics to prevent potential bacterial infections, anti-inflammatory drugs are also administered in current clinical treatments after cataract surgeries. Zhang *et al.* constructed a thermoresponsive nanocomposite formulation by incorporating prednisolone acetate-containing mesoporous silica nanoparticles (MSNs) into a levofloxacin-loaded thermogel matrix based on PLGA-PEG-PLGA.<sup>87</sup> MSNs act as an additional barrier that impedes the release of prednisolone acetate (PA) – a steroidal anti-inflammatory drug. *In vitro* release profiles were tuned such that a prolonged release of PA and short-term release of levofloxacin was achieved within a period of 28 days to adapt to the wound healing rates. When injected into the rabbit eye *via* subconjunctival injection, the nanocomposite thermogel depot provided outstanding antibiotic and anti-inflammatory effects for up to 21 days with only one-eighth of the initial cargo load of PA and levofloxacin. Thus, the nanocomposite thermogel formulation presents a promising single-dose drug delivery system to adopt after cataract surgery.

Although steroids reduce ocular inflammation, intraocular implants often induce elevated IOP. Ocular hypotensive agents, like beta-blocker levobunolol, can be administered to regulate IOP. Mohammadi *et al.* synthesized PLGA microparticles loaded with either levobunolol or dexamethasone and incorporated them into a thermogelling triblock copolymer consisting of poly (lactide-*co*-caprolactone) (PLCL) and PEG.<sup>88</sup> The triblock copolymer PLCL-PEG-PLCL could undergo sol-gel transition to form a depot when injected into the eye. Dexamethasone reduces inflammation, whereas levobunolol relieves IOP increase. In addition, moxifloxacin was directly encapsulated into the hydrogel matrix. This multi-drug thermogelling delivery platform demonstrated short-term slow release of moxifloxacin for up to 15 days for its antibiotic effects. At the same time, the thermogel provided a slower and prolonged release of dexamethasone and levobunolol for more than a month. Hydrophobic PLCL blocks in the thermogel contributed to the prolonged release rates of these biomolecules. Moreover, the ocular depot demonstrated the ability to tailor and optimize the release profiles of three different therapeutic drugs. This can be achieved by varying the initial drug load such that the drug dose released can be tuned while maintaining a constant release rate over time.

Yan *et al.* designed a different multi-drug thermogelling drug delivery system to be injected into the anterior chamber after cataract surgery to form an *in situ* gel depot that slowly releases antibiotics, steroids, and anti-PCO agents.<sup>89</sup> A Pluronic hydrogel matrix (26% F127/1.5% F68) was embedded with dexamethasone, moxifloxacin, and genistein-carrying mPEG-PLA functionalized nanostructured lipid carriers (GenNLC) (Fig. 11A). The final thermogelling composite demonstrated rapid gelation above 32 °C in 20.67 ± 0.5 s and exhibited good transparency of 93.44 ± 0.33% to 100% light







**Fig. 11** (A) Illustration of the Pluronic hydrogel matrix embedded with dexamethasone (Dex), moxifloxacin (Mox), and genistein-carrying mPEG-PLA functionalized nanostructured lipid carriers (GenNLC). The incorporation of Mox was coupled with CaCl<sub>2</sub>. (B) Transmittance of drug delivery systems with (purple) and without (blue) the thermogel. (C) Cumulative release of Mox (blue), Dex (red) and Genistein (yellow) from the thermogel for up to 40 days. Reproduced from ref. 89, used under Creative Commons CC-BY license 2021.

transmittance (Fig. 11B). Within 10 days, moxifloxacin was completely released from the depot (Fig. 11C). Meanwhile, dexamethasone experienced a burst release profile in the first week, followed by a sustained release for 30 days ( $97.14 \pm 3.38\%$ ), owing to the increase in crosslinking density provided by the addition of calcium ions. Simultaneously, genistein was gradually released at a decreasing rate with a cumulative released amount of  $63.35 \pm 2.49\%$  by day 40. *In vitro* studies revealed that the thermogel was able to effectively inhibit the proliferation, migration, and epithelial-mesenchymal transition of lens epithelial cells (SRA 01/04) in a dose-dependent manner. Taken together, this multi-drug release thermogelling depot potentially not only eliminates the need for post-operative application of ophthalmic drops, but also reduces posterior capsular opacification.

### 3.7. Dry eye disease from diabetes mellitus

DED is another common ocular complication that occurs in up to 54% of the diabetic population and its pathogenesis is rather multifactorial.<sup>138</sup> Chronic hyperglycaemia in diabetes contributes to several risk factors for DED, such as diabetic periphery neuropathy, reduced insulin levels, micro-vasculopathy, and systemic hyperosmolarity. These factors can induce lacrimal functional unit (LFU) dysfunction, abnormal tear dynamics and tear film dysfunction, which results in DED. Various proteins that are upregulated due to chronic hyperglycaemia have also been demonstrated to be implicated in the pathogenesis of DED. They include advanced glycation end product modified proteins, immune-inflammatory regulatory proteins, and LFU dysfunction-related proteins.<sup>139</sup>

Typically, patients with DED experience symptoms like compromised vision, irritation, and ocular pain, which reduce their quality of life.<sup>140</sup> In current clinical practice, topical application of eye drops is the gold standard intervention for DED as it is non-invasive and simple to perform. Nonetheless, as previously mentioned, any drug delivered *via* eye drops suffers from low bioavailability as they are rapidly cleared *via* tear dilution and the lacrimal drainage system.<sup>141</sup> As such, frequent application of eye drops is required to maintain the therapeutic concentration of the drug to alleviate DED.

Various thermogels have thus been developed to improve existing treatments for DED.

### 3.8. Thermogels for dry eye disease management

Luo *et al.* designed a long-acting mucoadhesive thermogel for the effective pharmacological treatment of DED.<sup>90</sup> They first synthesized thermoresponsive copolymers that are biodegradable by grafting PNIPAAm to gelatin (GN). Subsequently, the copolymer was modified with lectin Helix pomatia agglutinin (HPA) as a mucus-binding component. Finally, the thermogel formulation was loaded with epigallocatechin gallate (EGCG), which is a potential therapeutic agent for DED that elicits antioxidant and anti-inflammatory effects. Since the mucoadhesive property of the gel allows for strong adhesion to carbohydrates on the mucus layer of the tear film, the EGCG-loaded GN-HPA thermogel was able to form a stable drug delivery depot when injected *in situ* with prolonged residence time. Based on *in vivo* tests in a rabbit model of DED, a single-dose topical application of the EGCG-loaded GN-HPA thermogel onto the conjunctival sac provided sustained release of EGCG for over 14 days and efficaciously repaired corneal epithelial defects.

FK506-loaded ocular adhesive thermogels based on PEG-PPG copolymers modified with monofunctional polyhedral oligomeric silsesquioxane (MPOSS) have also been shown to be effective in alleviating DED in mice models (Fig. 12A).<sup>91</sup> FK506 is a hydrophobic macrolide immunosuppressant that is used in current clinical practice to relieve dry eyes, but it is highly hydrophobic with poor water solubility. By incorporating MPOSS blocks into the thermogelling copolymer, the water solubility of FK506 improved. In addition, MPOSS blocks contributed to the greater binding affinity of the thermogel to mucin, which enhanced their adhesion to the ocular surface. This allows the drug to retain on the ocular surface for extended periods of time (Fig. 12B) and thus, improving the resolution of dry eyes (Fig. 12C). Infiltration of CD4<sup>+</sup> T cells in the conjunctiva is usually a characteristic of dry eyes. Unlike other commercialised formulations of FK506 eye drops, *in vivo* experiments found that the treatment of dry eyes with FK506-loaded MPOSS-PEG-PPG thermogel was the most



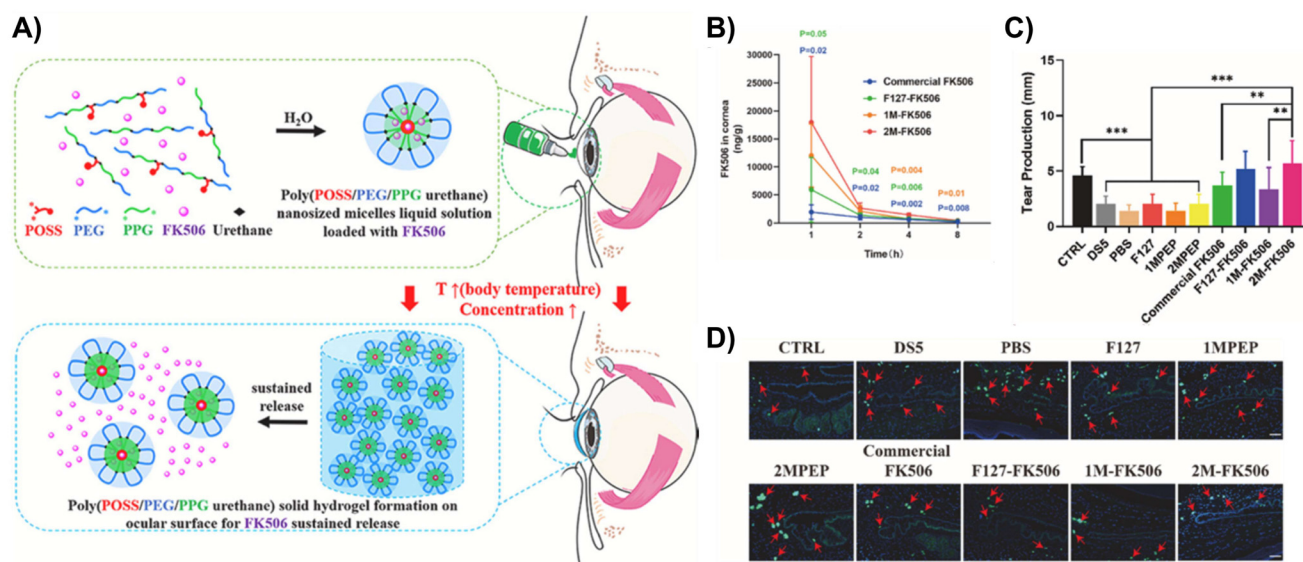


**Fig. 12** (A) Schematic of the self-assembly of FK506-loaded MPOSS-PEG-PPG (MPEP) thermogel, hydrogel formation and subsequent sustained release of FK506. (B) Based on ocular pharmacokinetics studies ( $n = 4$ , mean  $\pm$  S.E.M.), 2M-FK506 retained significantly higher drug concentrations in rabbit corneas for 8 h upon injection as compared to Commercial FK506 and F127-FK506. (C) As a result, topical administration of 2M-FK506 induced significantly higher tear production, which was measured via the phenol red thread test ( $n = 6$ ). (D) Histological images of the conjunctiva from *in vitro* tests on a dry eye murine model had CD4 staining, which shows the number and position of CD4<sup>+</sup> T cells infiltrating the conjunctiva from each group (red arrow indicates CD4<sup>+</sup> T cells). Ctrl = 0 mg mL<sup>-1</sup> FK506; DS5 = desiccating stress induced by scopolamine hydrobromide (0.25 g/100 mL); 1MPEP and 2MPEP = MPEP with 1 and 2 wt% MPOSS feed; 1M-FK506 = 1MPEP loaded with FK506; and 2M-FK506 = 2MPEP loaded with FK506. Reprinted from ref. 91, used under Creative Commons CC-BY-NC-ND 4.0 license 2022.

effective in suppressing CD4<sup>+</sup> T cells infiltrating the conjunctiva (Fig. 12D). Therefore, these findings showed that the addition of POSS blocks is promising for the development of thermogelling depots for the effective treatment of dry eyes.

Topical application of insulin is promising to promote corneal healing and reduce lesions in the lacrimal gland to prevent subsequent development of DED. Since most ophthalmic eye drops are ineffective to treat DED due to their poor bioavailability, Cruz-Cazarim *et al.* incorporated insulin-loaded chitosan microparticles (INS@CMP) into a thermogelling chitosan-poloxamer dispersion (C/P407) to improve the bioavailability of insulin delivery to the ocular surface and lacrimal gland.<sup>92</sup> Because of chitosan's mucoadhesive properties and penetrative abilities, chitosan microparticles can enable the slow release of insulin while minimizing immediate metabolism. In addition, by incorporating insulin-loaded chitosan microparticles into chitosan-poloxamer thermogels, the residence time of the gel depot formed on the ocular surface can be prolonged. As a result, *in vivo* studies revealed that diabetic rat dry eye models experienced an improvement in tear secretion by 77% within 5 days when instilled with the composite thermogel. In comparison, a lower tear secretion of 54% by day 5 was obtained when an aqueous solution of insulin was applied. After 15 days, no traces of insulin were found in the lacrimal gland and eyeball when treated with an aqueous solution of insulin, whereas significantly higher insulin concentration was detected when treated with INS@CMP/C/P407 as opposed to treatment with INS@C/407 and INS@CMP.

Overall, results showed that leveraging INS@CMP/C/P407 for insulin delivery had restored tear fluid volume and corneal thickness to healthy levels, protected corneal cell morphologies, and enhanced ocular bioavailability of insulin.

For moderate or severe cases where lubricating eye drops and gels are ineffective in alleviating DED, lacrimal drainage system occlusion is an alternative solution that extends the lubricant effects and preserves natural tears. Lin *et al.* prepared a thermogelling solution based on hydroxybutyl chitosan (HBC) for intracanalicular injection.<sup>94</sup> It can be easily injected into the lacrimal drainage system without spatial restrictions, which rapidly gel at physiological temperature into a resilient hydrogel that conforms to an individual's duct shape and functions as an absorbable intracanalicular plug (Fig. 13A). Moreover, the reduction in volume experienced by the HBC plug upon its sol-gel transition allowed the partial function of tear flow to be retained. Results showed a significant drop in flow flux of 76.9% occurring 10 minutes upon HBC injection and the effects of the HBC plug were sustained for over 4 weeks. Besides remarkable improvement in tear secretion observed in rabbit dry eye models (Fig. 13B), substantial improvement in ocular surface disease index (Fig. 13C) and tear break-up time (Fig. 13D) was reported from a pilot human trial with good compliance and no severe side effects.

Notably, inflammation is pervasive among patients with DED due to the continued activation and infiltration of pathogenic leukocytes into their ocular surface tissues. Accordingly,



**Fig. 13** (A) Thermogelling solution of HBC was administered via intracanalicular injection and gel to form a hydrogel plug at physiological temperature. (B) Phenol red thread test with rabbit dry eye models showed significant improvement in tear secretion of the HBC group as compared to the control group. \*Indicates  $p < 0.05$  compared to the control group. Upon HBC injection, a pilot human trial reported improvements in (C) ocular surface disease index and (D) tear break up time was reported from a pilot human trial. \*Indicates  $p < 0.05$  compared to the baseline. Reproduced from ref. 94 with permission from the Royal Society of Chemistry 2018.

treatment regimens for DED should also address potential adverse inflammatory responses. For this reason, Nguyen *et al.* developed a long-acting therapeutic thermogel with extended anti-inflammatory and corneal-protective effects.<sup>95</sup> To synthesize the thermogel, sulfated hyaluronic acid (sHA) was conjugated with amine-terminated PNIPAAm via EDC-NHS coupling. Owing to HA's strong dehydration resistance, potent anti-inflammatory effects, and good biocompatibility, HA was chosen for its therapeutic properties that can protect the corneal epithelium and ocular surface in addition to stabilizing the tear film in DED. Given that selectins are cell adhesion molecules that mediate leukocyte recruitment, functionalizing HA with selectin-binding groups, like sulfates, encourages strong electrostatic interactions with amino acid residues in selectin, perturbs binding affinity with cells in tissues and thereby inhibits selectin-mediated leukocyte infiltration. When the sHA-PNIPAAm copolymer was applied to the ocular surface, the solution transformed into a gel with prolonged residence time. Correspondingly, *in vivo* studies using rabbit dry eye models with a one-time topical application of the thermogel demonstrated ~99% repair of corneal epithelial defects, prevention of cellular apoptosis with ~68.3% cells recovered, and suppression of ocular surface inflammation by 4 folds within 7 days. Taken together, this thermogel presents great

promise as an efficient therapeutic agent that harnesses a unique approach of not only topically treating DED, but also mitigating potential inflammation mediated by leukocyte infiltration in DED.

## 4. Conclusion

Among the various types of physically crosslinked hydrogels, thermoresponsive hydrogels are particularly attractive for biomedical applications due to their ease of application, *in situ* gelation at physiological temperatures, high biocompatibility and tailorable properties. Over the past few decades, plenty of research studies have convincingly demonstrated the ability of thermogels to be utilized as drug depots for sustained drug delivery, vitreous substitutes, shape-conformable implants such as punctal plugs, and long-acting therapeutics. Translating thermogels into clinical settings could undoubtedly be a valuable and transformative factor in helping diabetics manage ocular diseases to which they are often predisposed. However, these research studies are in its infancy. In the ongoing development of thermogels, there are limitations that must be addressed to fully harness the potential of this valuable technology for clinical studies.





Thermogels have specific material requirements pertaining to each ophthalmic application they serve. For vitreous substitutes, achieving a balance between the gel's storage modulus and its opacity is imperative to ensure its suitability as a vitreous tamponade. This balance can be achieved by adjusting the molecular weight of the thermogelling polymer due to its influence on the physical and mechanical properties of the thermogel. In addition, the presence of multiple supramolecular interactions that existing injectable thermogels rely on also contributes to the physical and mechanical properties of the thermogel. However, the presence of these supramolecular interactions within thermogelling drug delivery depots can sometimes introduce complications in the delivery of therapeutic cargo. As therapeutic modalities expand beyond low molecular weight drugs to include nucleic acids, peptides, proteins, and antibodies, it is important to recognise their diverse physicochemical properties.<sup>142</sup> On that account, controlling drug release profiles in injectable thermogels becomes a significant challenge in the development of ophthalmic drug delivery systems. Overcoming this challenge requires translating materials research into real-life applications by taking external factors, such as drug incorporation and drug-polymer interactions, into consideration. These factors could influence the overall material structure, properties, and interactions with the drug, ultimately modifying drug release kinetics and therapeutic outcomes. Furthermore, formulation scientists need to tackle several other challenges related to the initial viscosity of the thermogel, biodegradability, sterilisation methods, storage conditions and ensuring long-term intraocular safety.

To date, there are no thermogels that have either been used clinically or undergoing clinical trials for ophthalmic applications. Nevertheless, various researchers are progressing their work on thermogels for ophthalmic applications towards clinical trials. Vitreogel® is a biodegradable thermogel that functions as a long-term vitreous substitute and prevents scarring of the retina as a result of failed retinal detachment repair surgeries. While the innovators of Vitreogel® are motivated to obtain regulatory approval from the Food and Drug Administration in the United States and Conformite Europeenne (CE) marking in Europe before advancing Vitreogel® to clinical trials in the next few years, they continue to evaluate the efficacy and safety of their thermogel using additional pre-clinical disease models.<sup>143,144</sup> At the same time, they are also establishing a manufacturing process to allow for polymer production at a large scale under current good manufacturing practice (cGMP) guidelines.<sup>145</sup> In most pre-clinical studies, formulation scientists often work with a small-scale synthesis of their thermogelling copolymers. To develop a large-scale production process for GMP production of thermogels for ophthalmic applications, several challenges, such as reproducibility, long-term stability, and batch-to-batch variations, need to be overcome by investing in time and advanced manufacturing technologies. Therefore, with continuous progress in thermogels for ophthalmic applications and the pursuit towards clinical application, we are assured that the emergence of a clinically-approved thermogel for the management of diabetic ocular diseases is just a matter of time.

## Author contributions

The manuscript was written through contributions of all authors, with equal contributions from co-first authors Nicholas Wei Xun Ong and Belynn Sim. All authors have read and approved the final version of the manuscript.

## Conflicts of interest

The authors declare no conflicts of interest.

## Acknowledgements

This research is supported by National Research Foundation (NRF) Singapore under its NRF Investigatorship (NRF-NRFI07-2021-0003), A\*STAR Central Research Fund, and funding from IAF-PP (A\*STAR, HBMS Domain) H20C6a0033 (OrBiTAL).

## References

- 1 H. Sun, P. Saeedi, S. Karuranga, M. Pinkepank, K. Ogurtsova, B. B. Duncan, C. Stein, A. Basit, J. C. N. Chan, J. C. Mbanya, M. E. Pavkov, A. Ramachandaran, S. H. Wild, S. James, W. H. Herman, P. Zhang, C. Bommer, S. Kuo, E. J. Boyko and D. J. Magliano, *Diabetes Res. Clin. Pract.*, 2022, **183**, 109119.
- 2 A. D. Association, *Diabetes Care*, 2009, **32**, S62–S67.
- 3 D. Tomic, J. E. Shaw and D. J. Magliano, *Nat. Rev. Endocrinol.*, 2022, **18**, 525–539.
- 4 G. A. Lutt, *Invest. Ophthalmol. Visual Sci.*, 2013, **54**, ORSF81–ORSF87.
- 5 N. Sayin, N. Kara and G. Pekel, *World J. Diabetes*, 2015, **6**, 92–108.
- 6 A. J. Lake, J. L. Browne, C. Abraham, D. Tumino, C. Hines, G. Rees and J. Speight, *BMC Health Serv. Res.*, 2018, **18**, 396.
- 7 M. J. Gale, B. A. Scruggs and C. J. Flaxel, *Clin. Exp. Ophthalmol.*, 2021, **49**, 128–145.
- 8 S. Z. Safi, R. Qvist, S. Kumar, K. Batumalaie and I. S. Ismail, *BioMed Res. Int.*, 2014, **2014**, 801269.
- 9 M. M. Marcet, R. M. Shtein, E. A. Bradley, S. X. Deng, D. R. Meyer, J. R. Bilyk, M. T. Yen, W. B. Lee and L. A. Mawn, *Ophthalmology*, 2015, **122**, 1681–1687.
- 10 G. Vrinda, S. Sadia, S. Jeff and P. Dhananjay, *J. Pharmacol. Exp. Ther.*, 2019, **370**, 602.
- 11 A. Farkouh, P. Frigo and M. Czejka, *Clin. Ophthalmol.*, 2016, **10**, 2433–2441.
- 12 K. G. Falavarjani and Q. D. Nguyen, *Eye*, 2013, **27**, 787–794.
- 13 K. Wang and Z. Han, *J. Controlled Release*, 2017, **268**, 212–224.
- 14 M. Fathi, J. Barar, A. Aghanejad and Y. Omidi, *BioImpacts*, 2015, **5**, 159–164.





- 15 H. Cao, L. Duan, Y. Zhang, J. Cao and K. Zhang, *Signal Transduction Targeted Ther.*, 2021, **6**, 426.
- 16 K. Zhang, K. Xue and X. J. Loh, *Gels*, 2021, **7**, 77.
- 17 J. Omar, D. Ponsford, C. A. Dreiss, T.-C. Lee and X. J. Loh, *Chem. – Asian J.*, 2022, **17**, e202200081.
- 18 X. Du, J. Zhou, J. Shi and B. Xu, *Chem. Rev.*, 2015, **115**, 13165–13307.
- 19 C. A. Dreiss, *Curr. Opin. Colloid Interface Sci.*, 2020, **48**, 1–17.
- 20 Q. Lin, C. Owh, J. Y. C. Lim, P. L. Chee, M. P. Y. Yew, E. T. Y. Hor and X. J. Loh, *Acc. Mater. Res.*, 2021, **2**, 881–894.
- 21 J. Shi, L. Yu and J. Ding, *Acta Biomater.*, 2021, **128**, 42–59.
- 22 G. Pasparakis and C. Tsitsilianis, *Polymer*, 2020, **211**, 123146.
- 23 R. Pelton, *J. Colloid Interface Sci.*, 2010, **348**, 673–674.
- 24 A. Halperin, M. Kröger and F. M. Winnik, *Angew. Chem., Int. Ed.*, 2015, **54**, 15342–15367.
- 25 X. Xu, Y. Liu, W. Fu, M. Yao, Z. Ding, J. Xuan, D. Li, S. Wang, Y. Xia and M. Cao, *Polymers*, 2020, **12**, 580.
- 26 S. S. Liow, Q. Dou, D. Kai, A. A. Karim, K. Zhang, F. Xu and X. J. Loh, *ACS Biomater. Sci. Eng.*, 2016, **2**, 295–316.
- 27 P. Singla, S. Garg, J. McClements, O. Jamieson, M. Peeters and R. K. Mahajan, *Adv. Colloid Interface Sci.*, 2022, **299**, 102563.
- 28 G.-E. Yu, Y. Deng, S. Dalton, Q.-G. Wang, D. Attwood, C. Price and C. Booth, *J. Chem. Soc., Faraday Trans.*, 1992, **88**, 2537–2544.
- 29 R. K. Prud'homme, G. Wu and D. K. Schneider, *Langmuir*, 1996, **12**, 4651–4659.
- 30 M. Nguyen-Misra and W. L. Mattice, *Macromolecules*, 1995, **28**, 1444–1457.
- 31 C.-L. Fu, Z.-Y. Sun and L.-J. An, *J. Phys. Chem. B*, 2011, **115**, 11345–11351.
- 32 M. A. da Silva, P. Haddow, S. B. Kirton, W. J. McAuley, L. Porcar, C. A. Dreiss and M. T. Cook, *Adv. Funct. Mater.*, 2022, **32**, 2109010.
- 33 Z. Gao, S. K. Varshney, S. Wong and A. Eisenberg, *Macromolecules*, 1994, **27**, 7923–7927.
- 34 L. Zhang and A. Eisenberg, *J. Am. Chem. Soc.*, 1996, **118**, 3168–3181.
- 35 S. Cui, L. Yu and J. Ding, *Macromolecules*, 2018, **51**, 6405–6420.
- 36 V. P. N. Nguyen, N. Kuo and X. J. Loh, *Soft Matter*, 2011, **7**, 2150–2159.
- 37 S. Cui, L. Yu and J. Ding, *Macromolecules*, 2019, **52**, 3697–3715.
- 38 B.-S. Chiou, S. R. Raghavan and S. A. Khan, *Macromolecules*, 2001, **34**, 4526–4533.
- 39 P. Lang and W. Burchard, *Macromolecules*, 1991, **24**, 814–815.
- 40 K. Xue, Z. Liu, Q. Lin, J. Y. C. Lim, K. Y. Tang, S. L. Wong, B. H. Parikh, X. Su and X. J. Loh, *ACS Appl. Bio Mater.*, 2020, **3**, 9043–9053.
- 41 E. A. Appel, X. J. Loh, S. T. Jones, C. A. Dreiss and O. A. Scherman, *Biomaterials*, 2012, **33**, 4646–4652.
- 42 M. M. Civan, in *The Eye's Aqueous Humor*, Academic Press, 2008, vol. 62, pp. 1–45.
- 43 F. Johnson and D. Maurice, *Exp. Eye Res.*, 1984, **39**, 791–805.
- 44 D. W. Smith, C.-J. Lee and B. S. Gardiner, *Prog. Retinal Eye Res.*, 2020, **78**, 100845.
- 45 X. J. Loh, P. L. Chee and C. Owh, *Small Methods*, 2019, **3**, 1800313.
- 46 K. Kanazaki, K. Sano, A. Makino, F. Yamauchi, A. Takahashi, T. Homma, M. Ono and H. Saji, *J. Controlled Release*, 2016, **226**, 115–123.
- 47 M. H. Park, M. K. Joo, B. G. Choi and B. Jeong, *Acc. Chem. Res.*, 2012, **45**, 424–433.
- 48 J. Sun, X. Liu, Y. Lei, M. Tang, Z. Dai, X. Yang, X. Yu, L. Yu, X. Sun and J. Ding, *J. Mater. Chem. B*, 2017, **5**, 6400–6411.
- 49 L. Zhang, W. Shen, J. Luan, D. Yang, G. Wei, L. Yu, W. Lu and J. Ding, *Acta Biomater.*, 2015, **23**, 271–281.
- 50 L. Chen, T. Ci, T. Li, L. Yu and J. Ding, *Macromolecules*, 2014, **47**, 5895–5903.
- 51 L. Yu, G. Chang, H. Zhang and J. Ding, *J. Polym. Sci., Part A: Polym. Chem.*, 2007, **45**, 1122–1133.
- 52 A. A. A. Smith, C. L. Maikawa, H. L. Hernandez and E. A. Appel, *Polym. Chem.*, 2021, **12**, 1918–1923.
- 53 Q. Lin, Z. Liu, D. S. L. Wong, C. C. Lim, C. K. Liu, L. Guo, X. Zhao, Y. J. Boo, J. H. M. Wong, R. P. T. Tan, K. Xue, J. Y. C. Lim, X. Su and X. J. Loh, *Biomaterials*, 2022, **280**, 121262.
- 54 Q. Lin, V. Ow, Y. J. Boo, V. T. A. Teo, J. H. M. Wong, R. P. T. Tan, K. Xue, J. Y. C. Lim and X. J. Loh, *Front. Bioeng. Biotechnol.*, 2022, **10**, 864372.
- 55 Q. Lin, J. Y. C. Lim, K. Xue, C. P. T. Chee and X. J. Loh, *RSC Adv.*, 2020, **10**, 39109–39120.
- 56 M. R. Matanović, J. Kristl and P. A. Grabnar, *Int. J. Pharm.*, 2014, **472**, 262–275.
- 57 S. Dai and K. C. Tam, *Langmuir*, 2004, **20**, 2177–2183.
- 58 M. Heskins and J. E. Guillet, *J. Macromol. Sci., Part A: Pure Appl. Chem.*, 1968, **2**, 1441–1455.
- 59 R. Hoogenboom, H. M. L. Thijs, M. J. H. C. Jochems, B. M. van Lankvelt, M. W. M. Fijten and U. S. Schubert, *Chem. Commun.*, 2008, **44**, 5758–5760.
- 60 J. Li and D. J. Mooney, *Nat. Rev. Mater.*, 2016, **1**, 16071.
- 61 C. Ding, L. Zhao, F. Liu, J. Cheng, J. Gu, S. Dan, C. Liu, X. Qu and Z. Yang, *Biomacromolecules*, 2010, **11**, 1043–1051.
- 62 T. Miao, S. L. Fenn, P. N. Charron and R. A. Floreani, *Biomacromolecules*, 2015, **16**, 3740–3750.
- 63 D. A. Prince, I. J. Villamagna, A. Borecki, F. Beier, J. R. de Bruyn, M. Hurtig and E. R. Gillies, *ACS Appl. Bio Mater.*, 2019, **2**, 3498–3507.
- 64 V. Ow, J. J. Chang, W. H. Chooi, Y. J. Boo, R. P. T. Tan, J. H. M. Wong, B. H. Parikh, X. Su, S. Y. Ng, X. J. Loh and K. Xue, *Carbohydr. Polym.*, 2023, **302**, 120308.
- 65 Y. Chen, Y. Li, W. Shen, K. Li, L. Yu, Q. Chen and J. Ding, *Sci. Rep.*, 2016, **6**, 31593.
- 66 S. Kim, H. J. Lee and B. Jeong, *Carbohydr. Polym.*, 2022, **291**, 119559.



- 67 Q. Lin, J. Y. C. Lim, K. Xue, X. Su and X. J. Loh, *Biomaterials*, 2021, **268**, 120547.
- 68 C. Mondelo-García, E. Bandín-Vilar, L. García-Quintanilla, A. Castro-Balado, E. M. del Amo, M. Gil-Martínez, M. J. Blanco-Teijeiro, M. González-Barcia, I. Zarra-Ferro, A. Fernández-Ferreiro and F. J. Otero-Espinar, *Macromol. Biosci.*, 2021, **21**, 2100066.
- 69 K. Xue, Z. Liu, L. Jiang, D. Kai, Z. Li, X. Su and X. J. Loh, *Biomater. Sci.*, 2020, **8**, 926–936.
- 70 S. Santhanam, J. Liang, J. Struckhoff, P. D. Hamilton and N. Ravi, *Acta Biomater.*, 2016, **43**, 327–337.
- 71 K. Xue, X. Zhao, Z. Zhang, B. Qiu, Q. S. W. Tan, K. H. Ong, Z. Liu, B. H. Parikh, V. A. Barathi, W. Yu, X. Wang, G. Lingam, W. Hunziker, X. Su and X. J. Loh, *Biomater. Sci.*, 2019, **7**, 4603–4614.
- 72 K. Zhang, Z. Liu, Q. Lin, Y. J. Boo, V. Ow, X. Zhao, D. S. L. Wong, J. Y. C. Lim, K. Xue, X. Su, D. Wu and X. J. Loh, *Biomater. Res.*, 2022, **26**, 70.
- 73 D. Park, V. Shah, B. M. Rauck, T. R. Friberg and Y. Wang, *Macromol. Biosci.*, 2013, **13**, 464–469.
- 74 C.-H. Wang, Y.-S. Hwang, P.-R. Chiang, C.-R. Shen, W.-H. Hong and G.-H. Hsiue, *Biomacromolecules*, 2012, **13**, 40–48.
- 75 B. Xie, L. Jin, Z. Luo, J. Yu, S. Shi, Z. Zhang, M. Shen, H. Chen, X. Li and Z. Song, *Int. J. Pharm.*, 2015, **490**, 375–383.
- 76 C. R. Osswald and J. J. Kang-Mieler, *Curr. Eye Res.*, 2016, **41**, 1216–1222.
- 77 C. R. Osswald, M. J. Guthrie, A. Avila, J. A. Valio Jr., W. F. Mieler and J. J. Kang-Mieler, *Curr. Eye Res.*, 2017, **42**, 1293–1301.
- 78 S. B. Turturro, M. J. Guthrie, A. A. Appel, P. W. Drapala, E. M. Brey, V. H. Pérez-Luna, W. F. Mieler and J. J. Kang-Mieler, *Biomaterials*, 2011, **32**, 3620–3626.
- 79 W. Liu, B. S. Lee, W. F. Mieler and J. J. Kang-Mieler, *Curr. Eye Res.*, 2019, **44**, 264–274.
- 80 W. Liu, A. P. Tawakol, K. M. Rudeen, W. F. Mieler and J. J. Kang-Mieler, *Transl. Vision. Sci. Technol.*, 2020, **9**, 13.
- 81 M. V. Fedorchak, I. P. Conner, J. S. Schuman, A. Cugini and S. R. Little, *Sci. Rep.*, 2017, **7**, 8639.
- 82 J. Sun, Y. Lei, Z. Dai, X. Liu, T. Huang, J. Wu, Z. P. Xu and X. Sun, *ACS Appl. Mater. Interfaces*, 2017, **9**, 7990–7999.
- 83 Y. H. Cheng, K. H. Hung, T. H. Tsai, C. J. Lee, R. Y. Ku, A. W. Chiu, S. H. Chiou and C. J. Liu, *Acta Biomater.*, 2014, **10**, 4360–4366.
- 84 I. S. Cho, C. G. Park, B. K. Huh, M. O. Cho, Z. Khatun, Z. Li, S.-W. Kang, Y. B. Choy and K. M. Huh, *Acta Biomater.*, 2016, **39**, 124–132.
- 85 A. Annala, B. C. Ilochonwu, D. Wilbie, A. Sadeghi, W. E. Hennink and T. Vermonden, *ACS Polym. Au*, 2023, **3**, 118–131.
- 86 Y.-H. Cheng, Y.-F. Chang, Y.-C. Ko and C. J.-L. Liu, *J. Biomed. Mater. Res., Part B*, 2020, **108**, 8–13.
- 87 S. Zhang, Y. Fang, J. Sun, Y. Deng and Y. Lu, *Adv. Ther.*, 2021, **4**, 2100088.
- 88 M. Mohammadi, K. Patel, S. P. Alaie, R. B. Shmueli, C. G. Besirli, R. G. Larson and J. J. Green, *Acta Biomater.*, 2018, **73**, 90–102.
- 89 T. Yan, Z. Ma, J. Liu, N. Yin, S. Lei, X. Zhang, X. Li, Y. Zhang and J. Kong, *Sci. Rep.*, 2021, **11**, 181.
- 90 L.-J. Luo, D. D. Nguyen and J.-Y. Lai, *Mater. Sci. Eng., C*, 2020, **115**, 111095.
- 91 Y. Han, L. Jiang, H. Shi, C. Xu, M. Liu, Q. Li, L. Zheng, H. Chi, M. Wang, Z. Liu, M. You, X. J. Loh, Y.-L. Wu, Z. Li and C. Li, *Bioact. Mater.*, 2022, **9**, 77–91.
- 92 E. L. C. Cruz-Cazarim, M. S. Cazarim, A. T. Ogunjimi, R. Petrilli, E. M. Rocha and R. F. V. Lopez, *Eur. J. Pharm. Biopharm.*, 2019, **140**, 1–10.
- 93 Z. Liu, S. S. Liow, S. L. Lai, A. Alli-Shaik, G. E. Holder, B. H. Parikh, S. Krishnakumar, Z. Li, M. J. Tan, J. Gunaratne, V. A. Barathi, W. Hunziker, R. Lakshminarayanan, C. W. T. Tan, C. K. Chee, P. Zhao, G. Lingam, X. J. Loh and X. Su, *Nat. Biomed. Eng.*, 2019, **3**, 598–610.
- 94 T. Lin, Y. Lu, X. Zhang, L. Gong and C. Wei, *Biomater. Sci.*, 2018, **6**, 3160–3169.
- 95 D. D. Nguyen, L.-J. Luo and J.-Y. Lai, *Mater. Today Bio*, 2022, **13**, 100183.
- 96 J. D. Steinmetz, R. R. A. Bourne, P. S. Briant, S. Flaxman, H. R. Taylor, J. B. Jonas, A. Abdoli, W. A. Abrha, A. Abualhasan, E. Abu-Gharbieh, T. G. Adal, A. Afshin, H. Ahmadi, W. Alemayehu, S. A. Alemzadeh, A. S. Alfaar, V. Alipour, S. Androudi, J. Arabloo, A. Arditi, B. B. Aregawi, A. Arrigo, C. Ashbaugh, E. Ashrafi, D. D. Atnafu, E. Bagli, A. A. Baig, T. W. Barnighausen, M. B. Parodi, M. Beheshti, A. S. Bhagavathula, N. Bhardwaj, P. Bhardwaj, K. Bhattacharyya, A. Bijani, M. Bikbov, M. Bottone, T. Braithwaite, A. M. Bron, S. B. Nagaraja, Z. A. Butt, F. L. C. dos Santos, V. L. A. Carneiro, R. J. Casson, C. Y. Cheng, J. Y. J. Choi, D. T. Chu, M. V. Cicinelli, J. M. Coelho, N. G. Congdon, R. A. S. Couto, E. A. Cromwell, S. M. A. Dahlawi, X. C. Dai, R. Dana, L. Dandona, R. Dandona, M. A. Del Monte, M. D. Molla, N. Derveniz, A. A. Desta, J. P. Deva, D. Diaz, S. Djalalinia, J. R. Ehrlich, R. Elayedath, H. R. Elhabashy, L. B. Ellwein, M. H. Emamian, S. Eskandarieh, F. Farzadfar, A. G. Fernandes, F. Fischer, D. S. Friedman, J. M. Furtado, S. Gaidhane, G. Gazzard, B. Gebremichael, R. George, A. Ghashghaee, S. A. Gilani, M. Golechha, S. Hamidi, B. R. Hammond, M. E. R. Hartnett, R. K. Hartono, A. Hashi, S. I. Hay, K. Hayat, G. Heidari, H. C. Ho, R. Holla, M. Househ, J. J. Huang, S. E. Ibitoye, I. M. Ilic, M. D. Ilic, A. D. Ingram, S. S. N. Irvani, S. M. S. Islam, R. Itumalla, S. Jayaram, R. P. Jha, R. Kahloun, R. Kalhor, H. Kandel, A. S. Kasa, T. Kavetsky, G. A. Kayode, J. H. Kempen, M. Khairallah, R. Khalilov, E. A. Khan, R. C. Khanna, M. N. Khatib, T. A. M. Khoja, G. R. Kim, J. E. Kim, Y. J. Kim, A. Kisa, S. Kisa, S. Kosen, A. Koyanagi, B. K. Bicer, V. Kulkarni, O. P. Kurmi, I. Landires, V. Lansingh, J. L. Leasher, K. E. LeGrand, N. Leveziel, H. Limburg, X. F. Liu, S. M. Kunjathur,



- S. Maleki, N. Manafi, K. Mansouri, C. McAlinden, G. G. Meles, A. M. Mersha, I. M. Michalek, T. R. Miller, S. Misra, Y. Mohammad, S. F. Mohammadi, J. A. Mohammed, A. H. Mokdad, M. A. Moni, A. Al Montasir, A. R. Morse, G. F. Mulaw, M. Naderi, H. Naderifar, K. S. Naidoo, M. D. Naimzada, V. Nangia, S. N. Swamy, M. Naveed, H. Negash, H. L. T. Nguyen, V. Nunez-Samudio, F. A. Ogbo, K. Ogundimu, A. T. Olagunju, O. E. Onwujekwe, N. Otstavnov, M. O. Owolabi, K. Pakshir, S. Panda-Jonas, U. Parekh, E. C. Park, M. Pasovic, S. Pawar, K. Pesudovs, T. Peto, H. Q. Pham, M. Pinheiro, V. Podder, V. Rahimi-Movaghar, M. H. U. Rahman, P. Y. Ramulu, P. Rath, D. L. Rawaf, S. Rawaf, L. Rawal, N. Reinig, A. M. N. Renzaho, A. Rezapour, A. L. Robin, L. Rossetti, S. Sabour, S. Safi, A. Sahebkar, M. A. Sahraian, A. M. Samy, B. Sathian, G. K. Saya, M. Saylan, A. A. Shaheen, M. A. Shaikh, T. T. Shen, K. Shibuya, W. S. Shiferaw, M. Shigematsu, J. I. Shin, J. C. Silva, A. Silvester, J. A. Singh, D. Singhal, R. S. Sitorus, E. Skiadaresi, V. Y. Skryabin, A. A. Skryabina, A. Soheili, M. B. Sorrie, R. Sousa, C. T. Sreeramareddy, D. Stambolian, E. G. Tadesse, N. Tahhan, M. I. Tareque, F. Topouzis, B. X. Tran, G. W. Tsegaye, M. K. Tsilimbaris, R. Varma, G. Virgili, A. Vongpradith, G. T. Vu, Y. X. Wang, N. L. Wang, A. H. Weldemariam, S. K. West, T. G. Wondmeneh, T. Y. Wong, M. Yaseri, N. Yonemoto, C. H. Yu, M. S. Zastrozhin, A. Zastrozhina, Z. J. Zhang, S. R. M. Zimsen, S. Resnikoff, T. Vos and Vision Loss Expert Group of the Global Burden of Disease Study, *Lancet Global Health*, 2021, **9**, e144–e160.
- 97 Z. L. Teo, Y. C. Tham, M. Yu, M. L. Chee, T. H. Rim, N. Cheung, M. M. Bikbov, Y. X. Wang, Y. T. Tang, Y. Lu, I. Y. Wong, D. S. W. Ting, G. S. W. Tan, J. B. Jonas, C. Sabanayagam, T. Y. Wong and C. Y. Cheng, *Ophthalmology*, 2021, **128**, 1580–1591.
- 98 D. A. Antonetti, P. S. Silva and A. W. Stitt, *Nat. Rev. Endocrinol.*, 2021, **17**, 195–206.
- 99 E. J. Duh, J. K. Sun and A. W. Stitt, *JCI Insight*, 2017, **2**(14), e93751.
- 100 T. Y. Wong, C. M. G. Cheung, M. Larsen, S. Sharma and R. Simó, *Nat. Rev. Dis. Primers*, 2016, **2**, 16012.
- 101 D. Călugăru and M. Călugăru, *Int. J. Ophthalmol.*, 2022, **15**, 1005–1010.
- 102 L. A. Everett and Y. M. Paulus, *Curr. Diabetes Rep.*, 2021, **21**, 35–35.
- 103 J. Wisniewska-Kruk, K. A. Hoeben, I. M. C. Vogels, P. J. Gaillard, C. J. F. Van Noorden, R. O. Schlingemann and I. Klaassen, *Exp. Eye Res.*, 2012, **96**, 181–190.
- 104 M. J. Elman, N. M. Bressler, H. Qin, R. W. Beck, F. L. Ferris, S. M. Friedman, A. R. Glassman, I. U. Scott, C. R. Stockdale and J. K. Sun, *Ophthalmology*, 2011, **118**, 609–614.
- 105 R. Rajendram, S. Fraser-Bell, A. Kaines, M. Michaelides, R. D. Hamilton, S. D. Esposti, T. Peto, C. Egan, C. Bunce, R. D. Leslie and P. G. Hykin, *Arch. Ophthalmol.*, 2012, **130**, 972–979.
- 106 M. Nauck, G. Karakiulakis, A. P. Perruchoud, E. Papakonstantinou and M. Roth, *Eur. J. Pharmacol.*, 1998, **341**, 309–315.
- 107 H. W. Kwak and D. J. D'Amico, *Arch. Ophthalmol.*, 1992, **110**, 259–266.
- 108 A. Mandal, D. Pal, V. Agrahari, H. M. Trinh, M. Joseph and A. K. Mitra, *Adv. Drug Delivery Rev.*, 2018, **126**, 67–95.
- 109 T. A. Bahr and S. J. Bakri, *Life*, 2023, **13**, 1098.
- 110 C. C. Wykoff, J. G. Garweg, C. Regillo, E. Souied, S. Wolf, D. S. Dhoot, H. T. Agostini, A. Chang, A. Laude, J. Wachtlin, L. Kovacic, L. Wang, Y. Wang, E. Bouillaud and D. M. Brown, *Am. J. Ophthalmol.*, 2023, DOI: [10.1016/j.ajo.2023.07.012](https://doi.org/10.1016/j.ajo.2023.07.012).
- 111 C. C. Wykoff, F. Abreu, A. P. Adamis, K. Basu, D. A. Eichenbaum, Z. Haskova, H. Lin, A. Loewenstein, S. Mohan, I. A. Pearce, T. Sakamoto, P. G. Schlottmann, D. Silverman, J. K. Sun, J. A. Wells, J. R. Willis, R. Tadayoni, T. Aaberg, A. Abbey, E. Abdulaeva, S. Abengoechea, P. Abraham, T. Ach, S. Adams, A. Adan Civera, S. Adrean, H. Agostini, S. Alam, A. Alezzandrini, V. Alfaro, D. Aliseda, A. Almony, P. Amat, P. Amini, A. Antoszyk, L. Arias, R. Asaria, M. Avila, C. C. Awh, J. Bafalluy, C. Baker, F. Bandello, M. Barakat, K. Barraza, G. Bator, C. Baumaal, R. Belfort Jr., C. Bergstrom, G. Bertolucci, T. Bochow, M. Bolz, E. Borcz, A. Bordon, D. Boyer, G. Bratko, M. Brent, J. Brown, D. M. Brown, M. Budzinskaya, S. Buffet, S. Burgess, B. Burton, M. Busquets, F. Cabrera, C. Cagini, J. Calzada, P. Campochiaro, J. Carlson, A. Castellarin, C. Cava, V. Chaikitmongkol, C. Chan, E. Chang, J. Chang, A. Chang, S. Charles, N. Chaudhry, C. Chee, J. Chen, F. Chen, S.-J. Chen, R. Cheong-Leen, A. Chiang, M. Chittum, D. Chow, B. Connolly, P. L. Cornut, K. Csaky, C. Danzig, A. Das, V. Daskalov, C. Desco, A. Dessouki, J. Dickinson, B. Do, M. Dollin, P. Dugel, J. Dusova, D. Eichenbaum, B. Eldem, R. Engstrom, J. Ernest, J. J. Escobar, S. Esposti, N. Eter, N. Falk, A. Farkas, L. Feiner, N. Feltgen, C. Fernandez, A. Fernandez Vega, P. Ferrone, J. Figueira, M. Figueroa, O. Findl, H. Fine, J. Fortun, G. M. Fox, S. Foxman, C. Framme, S. Fraser-Bell, A. Fu, A. Fukutomi, N. Fung, F. Furno Sola, R. Gallego-Pinazo, R. Garcia, A. Garcia-Layana, M. Gawecki, S. George, F. Ghanchi, G. Ghorayeb, R. Goldberg, M. Goldstein, N. Gomes, F. Gomez Ulla, V. Gonzalez, C. Greven, S. Gupta, M. Guzman, M. Harris, K. Hatz, V. Hau, V. Hau, K. Hayashi, J. Heier, E. Herba, V. Hersherberger, P. Higgins, A. Hirakata, A. Ho, N. Holekamp, S. Honda, J. Hsu, A. Hu, M. Hurcikova, Y. Ikeda, R. Isernhagen, Y. Ito, T. Jackson, R. Jacoby, A. Jafree, G. Javey, C. Javid, C. Jhaveri, M. Johnson, M. Kacerik, J. Kaluzny, D. Kampik, S. W. Kang, K. Kapoor, L. Karabas, T. Kawasaki, A. Kerenyi, A. Khanani, R. Khurana, B. Kim, K. Kimura, G. Kishino, S. Kitano, K. Klein-Mascia, G. Kokame, J. F. Korobelnik, A. Kulikov, A. Kuriyan, H. Kwong, R. Kwun, T. Lai, C.-C. Lai, P. Laird, L. Lalonde, P. Lanzetta, M. Larsen, C. Laugesen,



- D. Lavinsky, O. Lebreton, S. Lee, J. Levy, B. Lipkova, M. Liu, J. Liu, C. P. Lohmann, N. London, K. Lorenz, A. Lotery, D. Lozano Rechy, S. Lujan, P. Ma, T. Maeno, S. Mahmood, F. Makkouk, K. Malik, D. Marcus, A. Margherio, L. Mastropasqua, R. Maturi, F. McCabe, M. McKibbin, H. Mehta, G. Menon, J. Menten, K. Michalska-Malecka, A. Misheva, Y. Mitamura, P. Mitchell, Y. Modi, Q. Mohamed, J. Montero, J. Moore, V. Morales Canton, H. Morori-Katz, T. Morugova, T. Murakami, M. Muzyka-Wozniak, M. Nardi, J. Nemcansky, K. Nester-Ostrowska, J. Neto, C. Newell, M. Nicolo, J. Nielsen, K. Noda, A. Obana, N. Ogata, H. Oh, K. Oh, M. Ohr, P. Oleksy, S. Oliver, S. Olivier, J. Osher, S. Ozcaliskan, B. Ozturk, A. Papp, K. H. Park, D. W. Parke, M. C. Parravano, S. Patel, S. Patel, I. Pearce, J. Pearlman, F. Penha, I. Perente, S. Perkins, G. Pertile, I. Petkova, T. Peto, D. Pieramici, A. Pollreisz, P. Pongsachareonnont, N. Pozdeyeva, S. Priglinger, J. Qureshi, D. Raczynska, R. Rajagopalan, J. Ramirez Estudillo, P. Raskauskas, R. Rathod, H. Razavi, C. Regillo, F. Ricci, S. Rofagha, D. Romanczak, B. Romanowska-Dixon, D. Rosberger, I. Rosenblatt, B. Rosenblatt, A. Ross, P. Ruamviboonsuk, J. M. Ruiz Moreno, G. Salomão, S. Sandhu, D. Sandner, L. Sararols, O. Sawada, R. Schadlu, P. Schlottmann, C. Schuart, B. Seitz, A. Seres, F. Sermet, S. Shah, A. Shah, R. Shah, S. Sharma, T. Sheidow, V. Sheth, A. Shimouchi, M. Shimura, B. Sikorski, R. Silva, M. Singer, L. Singerman, R. Singh, E. Souied, D. J. Spinak, G. Spital, N. Steinle, J. Stern, G. Stoller, R. Stoltz, C. Stone, A. Stone, E. Suan, M. Sugimoto, I. Sugita, J. Sun, X. Sun, I. Suner, L. Szalczar, T. Szczesko, A. Tabassian, R. Tadayoni, H. Takagi, K. Takayama, A. Taleb, J. Talks, G. Tan, T. Tanabe, S. Taylor, A. Thach, J. Thompson, P. Tlucek, R. Torti, D. Tosheva Guneva, E. Toth-Molnar, E. Uchiyama, A. Vajas, D. Varma, B. Varsanyi, P. Vassileva, S. Vaz-Pereira, M. Veith, J. I. Vela, F. Viola, G. Virgili, G. Vogt, H. Vorum, P. Weber, T. Wecke, R. Wee, M. Weger, P. Weishaar, J. A. Wells, S. Wickremasinghe, T. R. Williams, T. Williams, G. Williams, A. Wolf, J. Wolfe, J. Wong, D. Wong, I. Wong, R. Wong, B. Wowra, C. C. Wykoff, E. Wylegała, C.-H. Yang, T. Yasukawa, P. Yates, G. Yilmaz, G. Yiu, Y. H. Yoon, B. Yoreh, S. Yoshida, H. G. Yu, S. Y. Yu, T. Yurieva, L. Zacharias, K. Zaczek Zakrzewska, A. Zambrano, B. Zatorska, C. Zeolite and J. Zheutlin, *Lancet*, 2022, **399**, 741–755.
- 112 I. Seah, X. Zhao, Q. Lin, Z. Liu, S. Z. Z. Su, Y. S. Yuen, W. Hunziker, G. Lingam, X. J. Loh and X. Su, *Eye*, 2020, **34**, 1341–1356.
- 113 F. E. Kane, J. Burdan, A. Cutino and K. E. Green, *Expert Opin. Drug Delivery*, 2008, **5**, 1039–1046.
- 114 A. Chan, L. S. Leung and M. S. Blumenkranz, *Clin. Ophthalmol.*, 2011, **5**, 1043–1049.
- 115 S. V. Ranade, M. R. Wieland, T. Tam, J. C. Rea, J. Horvath, A. R. Hieb, W. Jia, L. Grace, G. Barteselli and J. M. Stewart, *Drug Delivery*, 2022, **29**, 1326–1334.
- 116 A. Sharma, A. M. Khanani, N. Parachuri, N. Kumar, F. Bandello and B. D. Kuppermann, *Int. J. Retina Vitreous*, 2023, **9**, 6.
- 117 N. Celik, R. Khoramnia, G. U. Auffarth, S. Sel and C. S. Mayer, *Int. J. Ophthalmol.*, 2020, **13**, 1612–1620.
- 118 P. Le Bellec, P. Midoux, H. Cheradame, V. Bennevault and P. Guégan, *Eur. Polym. J.*, 2022, **168**, 111096.
- 119 B. Q. Y. Chan, H. Cheng, S. S. Liow, Q. Dou, Y.-L. Wu, X. J. Loh and Z. Li, *Polymers*, 2018, **10**, 89.
- 120 B. M. Rauck, T. R. Friberg, C. A. Medina Mendez, D. Park, V. Shah, R. A. Bilonick and Y. Wang, *Invest. Ophthalmol. Visual Sci.*, 2014, **55**, 469–476.
- 121 J. Cho, M. C. Heuzey, A. Bégin and P. J. Carreau, *Biomacromolecules*, 2005, **6**, 3267–3275.
- 122 H. Y. Zhou, L. J. Jiang, P. P. Cao, J. B. Li and X. G. Chen, *Carbohydr. Polym.*, 2015, **117**, 524–536.
- 123 N. Bhattarai, J. Gunn and M. Zhang, *Adv. Drug Delivery Rev.*, 2010, **62**, 83–99.
- 124 P. Cai and X. Chen, *ACS Mater. Lett.*, 2019, **1**, 285–289.
- 125 Q. Y. Gao, Y. Fu and Y. N. Hui, *Int. J. Ophthalmol.*, 2015, **8**, 437–440.
- 126 X. Su, M. J. Tan, Z. Li, M. Wong, L. Rajamani, G. Lingam and X. J. Loh, *Biomacromolecules*, 2015, **16**, 3093–3102.
- 127 B. H. Parikh, Z. Liu, P. Blakeley, Q. Lin, M. Singh, J. Y. Ong, K. H. Ho, J. W. Lai, H. Bogireddi, K. C. Tran, J. Y. C. Lim, K. Xue, A. Al-Mubaarak, B. Yang, R. Sowmiya, K. Regha, D. S. L. Wong, Q. S. W. Tan, Z. Zhang, A. D. Jeyasekharan, V. A. Barathi, W. Yu, K. H. Cheong, T. A. Blenkinsop, W. Hunziker, G. Lingam, X. J. Loh and X. Su, *Nat. Commun.*, 2022, **13**, 2796.
- 128 M. J. Ang and N. A. Afshari, *Clin. Exp. Ophthalmol.*, 2021, **49**, 118–127.
- 129 M. A. Javadi and S. Zarei-Ghanavati, *J. Ophthalmic Vision Res.*, 2008, **3**, 52–65.
- 130 Z. Kyselova, M. Stefek and V. Bauer, *J. Diabetes Complications*, 2004, **18**, 129–140.
- 131 H. Kiziltoprak, K. Tekin, M. Inanc and Y. S. Goker, *World J. Diabetes*, 2019, **10**, 140–153.
- 132 S. H. Chiou, C. J. Chang, C. K. Chou, W. M. Hsu, J. H. Liu and C. H. Chiang, *Diabetes Care*, 1999, **22**, 861–862.
- 133 Z. Hashim and S. Zarina, *Age*, 2011, **33**, 377–384.
- 134 Y. C. Liu, M. Wilkins, T. Kim, B. Malyugin and J. S. Mehta, *Lancet*, 2017, **390**, 600–612.
- 135 K. Kato, K. Miyake, K. Hirano and M. Kondo, *Cornea*, 2019, **38**(Suppl. 1), S25–S33.
- 136 V. P. Dave, J. Joseph, A. Pathengay, R. R. Pappuru and T. Das, *Retina*, 2020, **40**, 370–375.
- 137 J. A. An, O. Kasner, D. A. Samek and V. Lévesque, *J. Cataract Refractive Surg.*, 2014, **40**, 1857–1861.
- 138 L.-Y. Pan, Y.-K. Kuo, T.-H. Chen and C.-C. Sun, *Front. Med.*, 2022, **9**, 980714.
- 139 X. Zhang, L. Zhao, S. Deng, X. Sun and N. Wang, *J. Ophthalmol.*, 2016, **2016**, 8201053.
- 140 J. A. Clayton, *N. Engl. J. Med.*, 2018, **378**, 2212–2223.
- 141 R. Gaudana, J. Jwala, S. H. S. Boddu and A. K. Mitra, *Pharm. Res.*, 2009, **26**, 1197–1216.





- 142 A. M. Vargason, A. C. Anselmo and S. Mitragotri, *Nat. Biomed. Eng.*, 2021, 5, 951–967.
- 143 A\*STAR Research, A vision for better eye treatments, <https://research.a-star.edu.sg/articles/highlights/a-vision-for-better-eye-treatments/>, (accessed 15 September 2023).
- 144 BioSpectrum Asia, Singapore develops thermogel to prevent retinal scarring, <https://www.biospectrumasia.com/news/98/20637/singapore-develops-thermogel-to-prevent-retinal-scarring.html>, (accessed 15 September 2023).
- 145 X. Su, PVR: Saved by the Gel A hydrogel-based scarring solution for retinal detachment and beyond, <https://theophthalmologist.com/subspecialties/pvr-saved-by-the-gel>, (accessed 15 September 2023).

